Published for SISSA by Springer

Received: *April 10, 2026*
Accepted: *September 21, 2026*
Published: *October 15, 2026*

Particle transformers for identifying Lorentz-boosted Higgs bosons decaying to a pair of W bosons



The CMS collaboration

Full author list at the end of the paper

E-mail: cms-publication-committee-chair@cern.ch

Abstract: A novel deep neural network classifier, a "particle transformer" (ParT), is introduced for the identification of highly Lorentz-boosted resonances reconstructed as single, multipronged jets in measurements and searches performed by the CMS Collaboration at the CERN LHC. Based on a self-attention mechanism that allows the model to weigh the importance of different particles, ParT is trained on a wide variety of topologies, notably demonstrating strong performance for the first time on jets originating from boosted Higgs boson decays to W bosons. The ParT algorithm achieves a tagging efficiency of more than 50% for such jets at a background efficiency of 1%, while maintaining decorrelation from the jet mass. A calibration is performed in proton-proton collision data collected by CMS at a center-of-mass energy of 13 TeV, with a data set corresponding to a total luminosity of 138 fb^{-1}. Data-to-simulation selection efficiency scale factors are measured to be in the 0.9–1.0 range, with relative uncertainties between 7 and 23%. The tagging capability of ParT enhances the sensitivity of standard model measurements and searches for beyond-the-standard-model resonances decaying to hadronic diboson systems.

Keywords: Hadron-Hadron Scattering, Higgs Physics

ArXiv ePrint: 2604.09809

Open Access, Copyright CERN,
for the benefit of the CMS Collaboration.
Article funded by SCOAP^3.

https://doi.org/10.1007/JHEP10(2026)167

JHEP10(2026)167

Contents

1 Introduction 1

2 The CMS detector 3

3 Event reconstruction 3

4 Event simulation 5

5 The ParT algorithm 7
- 5.1 Model architecture and inputs 7
- 5.2 Model training 9
- 5.3 Performance of jet mass reconstruction 12

6 Performance and calibration of $H \to WW^*$ tagging 14
- 6.1 Performance 14
- 6.2 Mass decorrelation 17
- 6.3 Calibration using the Lund jet plane 18
- 6.4 Validation on jets from boosted top quark decays 22

7 Impact on measuring $HH \to b\bar{b}WW^*$ production properties 23

8 Summary 25

The CMS collaboration 34

JHEP10(2026)167

1 Introduction

Since discovering the Higgs boson (H) [1–3], the CMS and ATLAS Collaborations at CERN have been focused on precisely measuring its properties and interactions. Identifying its hadronic final states is an important avenue for doing so, as well as for searching for new physics processes. Traditionally, however, they have been considered challenging at a hadron collider because of the large background from standard model (SM) events composed uniquely of jets produced through the strong interaction, referred to as quantum chromodynamics (QCD) multijet events, as well as resonant processes such as top quark pair ($t\bar{t}$) production.

Over the past few years, the advent of progressively more advanced deep-learning (DL) techniques for jet identification, combined with the exploration of the highly Lorentz-boosted regime, has allowed the LHC experiments to steadily address this challenge. By exploiting the detailed low-level features of jets, including the kinematic, identification, and trajectory-related information of particle constituents and the presence and characteristics of secondary vertices, several DL algorithms have significantly improved our performance in tagging jets originating from decays of boosted resonances. These include DeepAK8 [4] and DeepDoubleX [5], which combine convolutional and recurrent neural networks; Xbb [6], which combines recurrent and feedforward neural networks; DeXTer [7], a deep-set-based neural network; and graph

neural network (GNN) architectures, such as interaction networks [8, 9], ParticleNet [10–12], and GN2X [13]. At a typical working point with a signal efficiency of about 50%, these advanced algorithms have improved background rejection by nearly an order of magnitude compared with simpler algorithms based on high-level jet features. They have been successfully employed to set some of the most stringent constraints on SM H to bottom quark ($H \to b\bar{b}$) decays in the gluon fusion (ggF) and vector boson fusion (VBF) production modes [14], the charm Yukawa coupling [15], H pair (HH) production, and the quartic coupling of two Higgs bosons and two weak (V) vector bosons HHVV [16, 17], as well as many beyond the SM (BSM) theories [18–23]. Beyond the LHC experiments, phenomenological studies with open data sets have studied a broad range of DL techniques for jet tagging, including image-based convolutional neural networks [24], set-based energy-flow networks [25], theory-inspired architectures [26], attention-based GNNs [27], Lorentz-equivariant neural networks [28–31], and transformer-based architectures [32].

These previous DL models have primarily focused on identifying *two-pronged* [33] large-radius jets, originating from the hadronization of two b or two c quarks produced in $H \to b\bar{b}$ and $H \to c\bar{c}$ decays. In this paper, we introduce a new model based on the particle transformer (ParT) architecture [32], and generalize it to identify large-radius jets with three or more prongs as well. These include the hadronic decay of $t \to Wb \to qqb$, and of the H to a W boson pair and then to four quarks, $H \to WW^* \to 4q$. Throughout this paper, $H \to WW^*$ denotes the SM decay, in which one of the two W bosons is off shell, while $H \to WW$ is used in the more general case where both W bosons may be either on or off shell, as for the Higgs boson-like scalars of varying mass used to train the algorithm (section 4). While three- and four-pronged jet taggers have been explored in phenomenological studies [34–38], the $H \to WW \to 4q$ topology in particular has seldom been probed experimentally at the LHC and only in the context of BSM searches [39]. Since the $H \to WW^* \to 4q$ decay has the second largest branching fraction after $H \to b\bar{b}$, this presents an opportunity to significantly constrain SM Higgs boson parameters, such as the quartic coupling between the Higgs and V boson, HHVV. It may also facilitate searches for a variety of new physics signatures, such as heavy Higgs bosons and two-Higgs-doublet models [40–42], where a large fraction of the signal exhibits a signature of a boosted W boson pair decaying hadronically, as well as BSM resonances decaying to boosted multiple vector boson systems [43–46].

Significant challenges to $H \to WW^*$ tagging include the need for stable performance across a wide range of jet masses (i.e., *mass decorrelation*), the asymmetric kinematic properties of the intermediate vector bosons, and the lack of a similar and abundant SM proxy for its calibration. The requirement of mass decorrelation enables searching for resonances in the jet mass distribution, while constraining backgrounds in data sidebands [47]. We address these challenges with a novel data generation and training scheme, and the use of a new calibration technique based on the primary Lund jet plane (LJP) [48, 49]. The calibration is performed in data collected in 2016–2018 with the CMS detector at the LHC in proton-proton (pp) collisions at a center-of-mass energy of 13 TeV, with a data set corresponding to an integrated luminosity of $138\,\text{fb}^{-1}$. Finally, we discuss an application of these techniques to the first search for SM HH production in the all-hadronic $b\bar{b}WW$ decay mode [50].

JHEP10(2026)167

The rest of this paper is organized as follows. Section 2 describes the CMS detector, section 3 explains the relevant event reconstruction algorithms, and section 4 details the event simulations used in this work. Section 5 then introduces the ParT model architecture, input features, and training, and section 6 presents its performance and calibration for $H \to WW^* \to 4q$ tagging compared with a previous state-of-the-art algorithm. Section 7 discusses its impact on the all-hadronic $HH \to b\bar{b}WW^*$ search. Finally, a summary is presented in section 8.

2 The CMS detector

The CMS apparatus [51, 52] is a multipurpose, nearly hermetic detector, designed to trigger on [53–55] and identify electrons, muons, photons, and (charged and neutral) hadrons [56–58]. Its central feature is a superconducting solenoid of 6 m internal diameter, providing a magnetic field of 3.8 T. Within the solenoid volume are a silicon pixel and strip tracker, a lead tungstate crystal electromagnetic calorimeter (ECAL), and a brass and scintillator hadron calorimeter (HCAL), each composed of a barrel and two endcap sections. Forward calorimeters extend the pseudorapidity (η) coverage provided by the barrel and endcap detectors. Muons are reconstructed using gas-ionization detectors embedded in the steel flux-return yoke outside the solenoid. More detailed descriptions of the CMS detector, together with a definition of the coordinate system used and the relevant kinematic variables, can be found in refs. [51, 52].

Events of interest are selected using a two-tiered trigger system. The first level, composed of custom hardware processors, uses information from the calorimeters and muon detectors to select events at a rate of around 100 kHz within a fixed latency of about 4 μs [53]. The second level, known as the high-level trigger, consists of a farm of processors running a version of the full event reconstruction software optimized for fast processing, and reduces the event rate to a few kHz before data storage [54].

The silicon tracker used in 2016 measured charged particles within the range $|\eta| < 2.5$. For nonisolated particles of $1 < p_T < 10$ GeV and $|\eta| < 1.4$, the track resolutions were typically 1.5% in p_T and 25–90 (45–150) μm in the transverse (longitudinal) impact parameter [58]. At the start of 2017, a new pixel detector was installed [59]; the upgraded tracker measured particles up to $|\eta| = 3.0$ with typical resolutions of 1.5% in p_T and 20–75 μm in the transverse impact parameter [60] for nonisolated particles of $1 < p_T < 10$ GeV. According to simulation studies [61], similar improvement is expected in the longitudinal direction.

3 Event reconstruction

The main physics objects of interest in this paper are large-radius jets that originate from the hadronic decays of boosted resonances and are reconstructed from the final-state particles produced in the pp collisions. Several different algorithms are used to reconstruct these jets, estimate their properties (such as their mass and momentum), identify their origin, and correct them for detector effects. This section briefly describes the relevant algorithms used in this paper.

A particle-flow (PF) algorithm [62] aims to reconstruct and identify each individual particle in an event, with an optimized combination of information from the various elements

JHEP10(2026)167

of the CMS detector. In this process, particles are identified exclusively as charged or neutral hadrons, photons, electrons, or muons, and are collectively referred to as PF candidates. The energy of photons is obtained from the ECAL measurement. The energy of electrons is determined from a combination of the electron momentum at the primary interaction vertex as determined by the tracker, the energy of the corresponding ECAL cluster, and the energy sum of all bremsstrahlung photons spatially compatible with originating from the electron track. The energy of muons is obtained from the curvature of the corresponding track. The energy of charged hadrons is determined from a combination of their momentum measured in the tracker and the matching ECAL and HCAL energy deposits, corrected for the response function of the calorimeters to hadronic showers. Finally, the energy of neutral hadrons is obtained from the corresponding corrected ECAL and HCAL energies. The primary vertex is taken to be the vertex corresponding to the hardest scattering in the event, evaluated using tracking information alone, as described in section 9.4.1 of ref. [63]. Secondary vertices (SVs), such as those found in b hadron decays, are reconstructed using the inclusive vertex finder algorithm, which identifies tracks with large impact parameters [64].

For each event, hadronic jets are clustered from these reconstructed particles using the infrared- and collinear-safe anti-k_{T} algorithm [65, 66] with a distance parameter of 0.4 (AK4 jets) or 0.8 (AK8 jets). Jet momentum is determined as the vector sum of all particle momenta in the jet, and is found from simulation to be, on average, within 5 to 10% of the true particle-level jet momentum over the whole p_{T} spectrum and detector acceptance. Additional pp interactions within the same or nearby bunch crossings (pileup) can contribute additional tracks and calorimetric energy depositions to the jet momentum. The charged-hadron subtraction [67] and pileup-per-particle identification (PUPPI) [68, 69] algorithms are used to mitigate the effect of pileup on AK4 and AK8 jets, respectively. In the PUPPI algorithm, charged particles identified as originating from pileup vertices are removed, while each neutral particle is assigned a probability weight indicating its likelihood of originating from the primary vertex. The AK8 jets are then clustered using the output PF candidate list, where the four-momenta of each particle are reweighted accordingly. For both jet types, jet energy corrections derived from simulation ensure that the average measured jet energies are aligned with those of particle-level jets. To account for residual differences between data and simulation in the jet energy scale, in situ momentum balance measurements are performed in dijet, photon+jet, Z+jet, and multijet events, with appropriate corrections applied based on these results [70].

To identify subjets within AK8 jets for the LJP calibration procedure described in section 6, the reconstructed jet constituents are reclustered using the exclusive-k_{T} algorithm [71, 72], which uses a target number of subjets as its stopping criterion rather than a distance parameter. The exclusive-k_{T} algorithm was found in ref. [49] to be more effective at identifying subjets than the Cambridge-Aachen [73, 74] and anti-k_{T} algorithms widely used in similar analyses. Following ref. [49], the reclustered subjets have their energies corrected using the same factors applied to the respective AK8 jets, and their k_{T} clustering history is used to measure their LJP.

Two algorithms are used in this paper to calculate the mass of AK8 jets for comparisons with ParT. The first is the soft-drop (SD) algorithm [75], with parameters $z = 0.1$ and $\beta = 0$, which prunes soft and collinear radiation from the jet. The algorithm outputs two

JHEP10(2026)167

subjets, whose invariant mass is taken to be the SD mass (m_{SD}). The second is a mass regression algorithm using the ParticleNet architecture, which leverages PF candidate and SV information in a GNN to predict the jet mass (m_{reg}), and has demonstrated improved mass resolution of two-pronged jets compared with the SD mass with the aforementioned parameters [12]. The DeepJet recurrent neural network algorithm [76] is used to identify AK4 jets originating from b quarks, as discussed in section 6.

The missing transverse momentum vector $\vec{p}_{\mathrm{T}}^{\,\mathrm{miss}}$ is computed as the negative vector sum of the transverse momenta of all the PF candidates in an event, and its magnitude is denoted as $p_{\mathrm{T}}^{\mathrm{miss}}$ [77]. The $\vec{p}_{\mathrm{T}}^{\,\mathrm{miss}}$ is modified to account for corrections to the energy scale of the reconstructed jets in the event.

4 Event simulation

The ParT algorithm is trained on simulated signal events containing jets from boosted Higgs boson-like decays and background events with top quark-like or QCD jets. During training, it is essential that a wide range of jet masses and momenta are included, as described in section 5.2, to ensure ParT does not learn to identify specific resonance masses or p_{T} ranges, thereby decorrelating the tagger output from jet mass and p_{T}. This decorrelation is necessary to search for resonances in the jet mass distribution, where it is important that the tagger does not artificially sculpt the background jet mass distribution to mimic the signal, thereby introducing a potential bias in the search. Several decorrelation approaches have been proposed in the literature, including adversarial training [78–80], variable transformation [47], quantile regression [9], and dedicated loss function penalty terms [81]. In this work, we instead rely on the generation of a broad range of signal resonance masses, thus implicitly training the tagger to be less sensitive to specific mass values [11]. Higgs boson-like and top quark-like topologies are simulated using, respectively, a spin-2 resonance G decaying to HH and a spin-0 resonance S decaying to $\mathrm{t\bar{t}}$, with the masses of the G, H, S, and t resonances varied as described below. We exclusively consider AK8 jets in model training and evaluation. To simplify the data set generation, all events are simulated under the 2017 data-taking conditions. However, the performance of ParT trained using these samples has been verified to be consistent when applied to data collected in 2016, 2017, and 2018. The algorithm is calibrated separately for each data-taking period and is applied to the full Run 2 dataset.

The H jet topology is simulated via $\mathrm{G} \to \mathrm{HH}$, generated with MadGraph5_aMC@NLO 2.6.5 [82] at leading order (LO). The jet p_{T} and mass ranges are controlled by varying the G mass (m_{G}) from 600 to 6000 GeV in 100 GeV increments, and the Higgs boson mass (m_{H}) from 15 to 250 GeV in 5 GeV increments for $m_{\mathrm{H}} < 50$ GeV and 10 GeV increments for $m_{\mathrm{H}} > 50$ GeV. The G boson width is set to 1 MeV, while the narrow width approximation (NWA) is applied to the Higgs boson. The H decays are simulated with JHUGen 7.1.4 [83] for $\mathrm{H} \to \mathrm{WW}^* \to 4\mathrm{q}$ or $\ell\nu\mathrm{qq}$ decay processes, and with pythia 8.205 for $\mathrm{H} \to \mathrm{b\bar{b}}$, $\mathrm{H} \to \mathrm{c\bar{c}}$, $\mathrm{H} \to \mathrm{s\bar{s}}$, $\mathrm{H} \to \mathrm{q\bar{q}}$, and $\mathrm{H} \to \tau^+\tau^-$ decays. The ratio of the W boson mass (m_{W}) to m_{H} is kept fixed to the SM value of 0.64 [84] for each m_{H} point. This ensures that one of the intermediate W bosons is on-shell while the other is off-shell, which improves the mass decorrelation and performance on the SM $\mathrm{H} \to \mathrm{WW}^*$ topology, as described in section 5.2. While m_{W} in principle affects

JHEP10(2026)167

the relative branching fractions of the $H \to WW^* \to 4q$ and $\ell\nu qq$ decay modes, the two processes are generated separately in equal proportion.

The t jet topology is simulated using $S \to t\bar{t}$, generated with MadGraph5_aMC@NLO 2.6.5 at LO. The masses of the S boson (m_S) and the top quark (m_t) are varied as in the H jet setup, with the widths set to 1% of m_S for the S boson and the NWA for the top quark. The W boson decays are simulated at the matrix element level, with the m_W again configured such that $m_W/m_t = 0.47$, i.e., at the SM value [84]. This setup improves the decorrelation of t tagging performance from the jet mass, while maintaining sensitivity to the top quark jet background characteristic of the SM configuration. Unlike the $H \to WW^* \to 4q$ case, where the tagger is optimized specifically for the SM $H \to WW^*$ decay topology, we additionally smear m_W/m_t. This is achieved by setting the width of the W boson equal to m_W, i.e., significantly larger than its SM value, resulting in the m_W being more varied across events. This further improves the sensitivity to BSM top quark-like decays where the ratio m_W/m_t may be different from the SM value. The G and S particles are used purely as convenient means to produce and control the kinematic properties of H and t jets and do not otherwise influence ParT training. In this section, H denotes a Higgs boson-like scalar that decays through the same modes as the SM Higgs boson but whose mass is varied over the range given in table 1, and t likewise denotes a top quark-like particle of varying mass. The symbol Y is instead reserved for the BSM scalar resonances considered in section 6.1, following the convention of CMS searches for $X \to HY$. The masses of the particles considered in H and t jet simulations are summarized in table 1.

The QCD multijet events are simulated at LO using pythia 8.205 [85] with the jet p_T sampled from different ranges to ensure broad coverage in jet mass and p_T. The "ghost association" method [86] is employed to determine the flavor of the partons that produce the jets, wherein reconstructed jets are reclustered with the final generated b or c hadrons in their decay chains. Their four-momenta are adjusted to preserve only directional information without affecting the jet momentum. The jet origin is determined by counting the number of ghost-associated b or c hadrons. Jets originating from resonant boosted Higgs bosons and top quarks are categorized according to the number and flavor of daughter quarks falling within the reconstructed AK8 jet.

Additional independent test samples are generated with SM $H \to WW^*$ and $t\bar{t}$ jet topologies to evaluate the performance of ParT for SM searches. The Higgs boson topology for testing is produced through a similar process to that for the training sample, but with m_G fixed at 1000 GeV and SM values for m_H and m_W. The SM top quark-like jets are simulated using the same resonant $t\bar{t}$ process, with m_S ranging from 1200 to 4500 GeV. The parameters m_W, m_t, and the W boson width are all fixed to their SM values. Finally, the performance is evaluated for BSM signals of scalar bosons (Y) decaying to SM W bosons as well, for searches for new Higgs boson-like resonances away from the SM m_H. These are simulated similarly to the H jet training samples, with G decaying to HY and m_G and the Y mass (m_Y) varying, but the Y decaying to the SM W bosons.

The calibration of ParT is demonstrated on simulated HH events in section 7. Production via the ggF channel is simulated at next-to-LO (NLO) accuracy in perturbative QCD using powheg 2.0 [87–90], whereas the VBF channel is simulated at LO using Mad-

JHEP10(2026)167

H jets ($G \to HH$)		t jets ($S \to t\bar{t}$)	
m_G	600–6000 GeV	m_S	600–6000 GeV
m_H	15–250 GeV	m_t	15–250 GeV
m_W	Fixed to SM ratio: $0.64m_H$	m_W	Fixed to SM ratio: $0.47m_t$
All other particles: SM values			

Table 1. Summary of particle masses in the ParT training samples.

Graph5_aMC@NLO 2.6.5 [82] because the corresponding NLO corrections are small [91]. A basis of samples is simulated with different κ_{2V}, κ_λ, and κ_V coupling modifiers and linear combinations of these are used to model all possible variations. The parameter κ_λ is the coupling modifier of the Higgs boson trilinear self-interaction, κ_{2V} the interaction between two vector bosons and two Higgs bosons, and κ_V the interaction between a Higgs boson and two vector bosons. In this work, these additional samples are used to demonstrate the stability of the LJP calibration procedure.

The production cross sections of the ggF samples are normalized to the next-to-NLO (NNLO) predictions for each coupling value [92–98], whereas the SM VBF production cross section is normalized to the prediction at next-to-NNLO (N^3LO) in QCD [91] with the same N^3LO/LO correction applied to all other couplings.

For all processes in this paper, the parton showering, hadronization, and underlying event interactions are simulated using pythia 8.205 [85] with the CP5 [99] tune. The parton distribution functions used correspond to those from NNPDF 3.0 [100] and 3.1 [101]. The response of the CMS detector is modeled with the Geant4 package [102], with pileup included by overlaying simulated minimum bias interactions on the hard scattering process.

5 The ParT algorithm

The ParT algorithm is an AK8 jet tagger and jet mass regressor that incorporates a dedicated $H \to WW^*$ classification node while achieving decorrelation with the jet mass. It is a self-attention-based model that is trained to distinguish between QCD jets and a variety of hadronically and leptonically decaying H and t jets for general use beyond $H \to WW^*$ identification, as well as to better estimate the jet mass. This section describes the ParT model, including training samples, input features, model architecture, training procedures, and performance benchmarks.

5.1 Model architecture and inputs

We employ a particle transformer architecture, which has been shown to achieve state-of-the-art performance on large-scale data sets [32], outperforming convolutional and graph neural networks, such as ParticleNet, with similar computational efficiencies. The ParT algorithm processes input particles and vertices as a permutation-invariant set of tokens, updating each particle's features through a series of modified multi-head self-attention blocks, referred to as "particle attention blocks" (PABs). Beyond the standard self-attention mechanism [103], which allows the model to weigh the importance of different inputs when updating their

JHEP10(2026)167

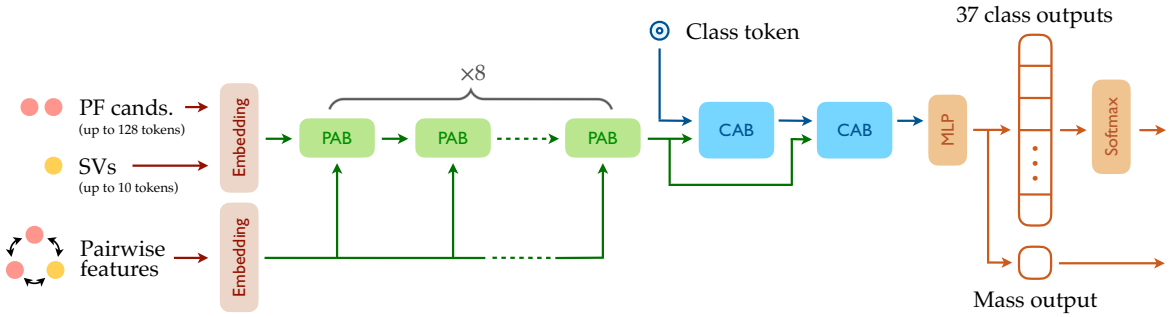


Figure 1. Diagram of the ParT model architecture. The model processes two different sets of input features per jet, from PF candidates and SVs. These features are embedded using separate MLPs into 128-dimensional representations before being concatenated and passed through eight PABs. Pairwise features are also calculated between each input element, which are embedded using a single one-dimensional convolutional layer and used as attention biases for each PAB. Two CABs then use the learned features to update a randomly initialized class token, which aggregates these features into a global representation of the jet. Their output is then finally passed through an MLP that outputs the class probabilities, which are normalized by a softmax function, as well as the jet mass.

collective representations, PABs incorporate pairwise features between the input particles and vertices that are embedded and used as attention biases in each block. After eight PABs, two more class attention blocks (CABs) [104] use the learned features to update a randomly initialized class token, which aggregates these features into a global representation of the jet. This class token is then passed through a final multi-layer perceptron (MLP) that outputs the class probabilities, which are normalized by a softmax function [105], and the jet mass as an auxiliary training objective (as discussed in section 5.2). In this way, the model employs a unified backbone that jointly performs jet tagging and jet mass regression while maintaining the performance of both tasks. A diagram of the architecture is shown in figure 1.

Transformers are also more computationally efficient than GNNs. The ParT model has a significantly larger capacity than the ParticleNet model of refs. [11, 12], with 2.3 million parameters compared with 500,000. However, its inference time is 6% smaller than that of ParticleNet. The ParT model has also been shown to require fewer floating point operations per inference than comparable ParticleNet models [32].

A distinguishing feature of our algorithm with respect to ref. [32] is the use of two different sets of input features: PF candidates and SVs within the jet. All jets are used, but the number of input elements per jet is capped. Based on the distributions of their multiplicities, we select up to 128 PF candidates and 10 SVs per jet. These limits are chosen to be large enough that, for more than 99.5% of jets, every reconstructed PF candidate and SV is passed to the network. For the small fraction of jets whose multiplicities exceed these limits, only the highest-p_{T} objects are retained. The PF candidates, including both charged and neutral particles, are taken as constituents of the AK8 jet. Their input features include kinematic information, particle charge and type, as well as trajectory-related properties in the case of charged particles. Properties of SVs whose momentum direction lies within the jet, such as kinematic information and impact parameters, are also included as input features. The full set of features is listed in table 2. The features of both data groups are embedded using

JHEP10(2026)167

separate MLPs into 128-dimensional representations before being concatenated and passed through the PABs. All input features are preprocessed such that their means and standard deviations across the training distributions are approximately 0 and 1, respectively.

Pairwise features $\ln\Delta, \ln(k_\mathrm{T}/\mathrm{GeV}), \ln z$, and $\ln(m^2/\mathrm{GeV}^2)$ are calculated between all input elements from their four-momenta [26], where

$$\Delta = \sqrt{(\Delta y)^2 + (\Delta\phi)^2}, \tag{5.1}$$

$$k_\mathrm{T} = \min(p_{\mathrm{T},a}, p_{\mathrm{T},b})\Delta, \tag{5.2}$$

$$z = \min(p_{\mathrm{T},a}, p_{\mathrm{T},b})/(p_{\mathrm{T},a} + p_{\mathrm{T},b}), \tag{5.3}$$

$$m^2 = (E_a + E_b)^2 - \|\mathbf{p}_a + \mathbf{p}_b\|^2, \tag{5.4}$$

Δy and $\Delta\phi$ are the pairwise differences in rapidity and the azimuthal angle, respectively; $p_{\mathrm{T},i} = (p_{x,i}^2 + p_{y,i}^2)^{1/2}$ is the transverse momentum; and $\mathbf{p}_i = (p_{x,i}, p_{y,i}, p_{z,i})$ is the momentum 3-vector and $\|\cdot\|$ is the norm, for $i = a, b$. These features are embedded into a 64-dimensional representation using one-dimensional convolutional layers and then used as attention biases for each PAB. These architectural hyperparameters are based on those in ref. [32].

5.2 Model training

The final states for each topology are categorized by the number of quarks and leptons per jet, and then further separated by flavor. Notably, jets from fully hadronic $\mathrm{H} \to \mathrm{WW}^*$ decays are separated into 4- and 3-pronged jets (4q and 3q), where the 3-pronged jet category corresponds to the case where one of the four WW^* daughter quarks falls outside of the jet cone. Other Higgs boson decay modes, including $\mathrm{H} \to \mathrm{qq}$ and $\mathrm{H} \to \tau\tau$, are also targeted for applications to other CMS searches, which will be the subject of future work. The full set of training classes is shown in figure 2.

The primary goal of ParT is jet classification among these 37 classes, along with an auxiliary task of regressing the jet mass. The classification task uses a cross-entropy loss function, while the mass regression task uses the "log-cosh" loss:

$$\mathcal{L}_{\text{log-cosh}}(m_\text{true}, m_\text{pred}) = \ln(\cosh((m_\text{pred} - m_\text{true})/\mathrm{GeV})), \tag{5.5}$$

where m_true is chosen to be the resonance mass, m_H or m_t, for H and t jets, and the generator-level m_SD for QCD jets, as described in ref. [12], expressed in units of GeV. The log-cosh function smoothly interpolates between the mean squared error for small differences and mean absolute error for large differences, and has been shown to achieve superior performance for jet mass regression, while being less sensitive to outliers [12]. The overall training objective is to minimize the sum of the cross-entropy and log-cosh losses simultaneously, with the log-cosh loss weighted by a hyperparameter λ to balance the two objectives. The value of λ has been tuned empirically to 0.05.

The ParT algorithm is trained to be decorrelated with the jet mass firstly by varying m_H and m_t in the training samples, as described in section 4. For H decays into light SM particles, i.e., quarks and τ leptons, varying m_H alone is sufficient to achieve mass decorrelation, while maintaining strong tagging performance, as illustrated by studies of the ParticleNet algorithm [11, 12]. However, the high mass of the W boson poses a challenge

JHEP10(2026)167

Variable	Definition
	PF candidates
$\ln(p_T/\text{GeV})$	Logarithm of the particle p_T
$\ln(E/\text{GeV})$	Logarithm of the particle energy
$\Delta\eta$(jet)	Difference in pseudorapidity between the particle and the jet axis
$\Delta\phi$(jet)	Difference in azimuthal angle between the particle and the jet axis
$\lvert\eta\rvert$	Absolute value of the particle pseudorapidity
q	Electric charge of the particle
`isMuon`	True if the particle is identified as a muon
`isElectron`	True if the particle is identified as an electron
`isChargedHadron`	True if the particle is identified as a charged hadron
`isPhoton`	True if the particle is identified as a photon
`isNeutralHadron`	True if the particle is identified as a neutral hadron
`pvAssociationQuality`	Quality of the association of the track to the primary vertices $^{(\star)}$
`lostInnerHits`	Quality of the track related to missing hits on the pixel layers $^{(\star)}$
χ^2/ndof	The χ^2 value of the trajectory fit normalized to the number of degrees of freedom $^{(\star)}$
`qualityMask`	Quality of the track $^{(\star)}$
d_z	Longitudinal impact parameter of the track $^{(\star)}$
d_z/σ_{d_z}	Significance of the longitudinal impact parameter $^{(\star)}$
d_{xy}	Transverse impact parameter of the track $^{(\star)}$
$d_{xy}/\sigma_{d_{xy}}$	Significance of the transverse impact parameter $^{(\star)}$
η_{rel}	Pseudorapidity of the track relative to the jet axis $^{(\star)}$
$p_{\text{T,rel}}$ ratio	Relative track momentum perpendicular to the jet axis $^{(\star)}$
$p_{\text{par,rel}}$ ratio	Relative track momentum parallel to the jet axis $^{(\star)}$
d_{3D}	Signed three-dimensional (3D) impact parameter of the track [106] $^{(\star)}$
d_{3D}/σ_{3D}	Signed 3D impact parameter significance of the track $^{(\star)}$
`trackDistance`	Distance between the track and jet axis at the point of closest approach $^{(\star)}$
	Secondary vertices within the jet
$\ln(p_T/\text{GeV})$	Logarithm of the SV p_T, defined as the p_T of the vector sum of the tracks associated with the SV
m_{SV}	Invariant mass of the tracks associated with the SV
$\Delta\eta$(jet)	Difference in pseudorapidity between the SV and the jet axis
$\Delta\phi$(jet)	Difference in azimuthal angle between the SV and the jet axis
$\lvert\eta\rvert$	Absolute value of the SV pseudorapidity
N_{tracks}	Number of tracks associated with the SV
χ^2/ndof	The χ^2 value of the SV fit normalized to the number of degrees of freedom
d_{2D}	Signed two-dimensional (2D) impact parameter of the SV
d_{2D}/σ_{2D}	Signed 2D impact parameter significance of the SV
d_{3D}	Signed 3D impact parameter of the SV
d_{3D}/σ_{3D}	Signed 3D impact parameter significance of the SV

Table 2. The complete set of input features per AK8 jet used for the ParT model training. Two types of inputs are considered: PF candidates and secondary vertices (SVs). The PF candidate features marked with a star ($\star$) apply only to charged PF candidates and a null value is used for neutral candidates.

JHEP10(2026)167

Process	Final state		Flavor	Classes
H→WW* (all-hadronic)	$q\bar{q}q\bar{q}$	⊗	0c / 1c / 2c	3
	$q\bar{q}q$			3
H→WW* (semileptonic)	$e\nu q\bar{q}$	⊗	0c / 1c	2
	$\mu\nu q\bar{q}$			2
	$\tau_e\nu q\bar{q}$			2
	$\tau_\mu\nu q\bar{q}$			2
	$\tau_h\nu q\bar{q}$			2
H→$q\bar{q}$			$b\bar{b}$	1
			$c\bar{c}$	1
			$s\bar{s}$	1
			$q\bar{q}$ (q=u/d)	1
H→ττ	$\tau_e\tau_h$			1
	$\tau_\mu\tau_h$			1
	$\tau_h\tau_h$			1
t→bW (hadronic)	$bq\bar{q}$	⊗	1b + 0c / 1c	2
	bq			2
t→bW (leptonic)	$be\nu$	⊗	1b	1
	$b\mu\nu$			1
	$b\tau_e\nu$			1
	$b\tau_\mu\nu$			1
	$b\tau_h\nu$			1
QCD			b	1
			$b\bar{b}$	1
			c	1
			$c\bar{c}$	1
			others (udsg)	1

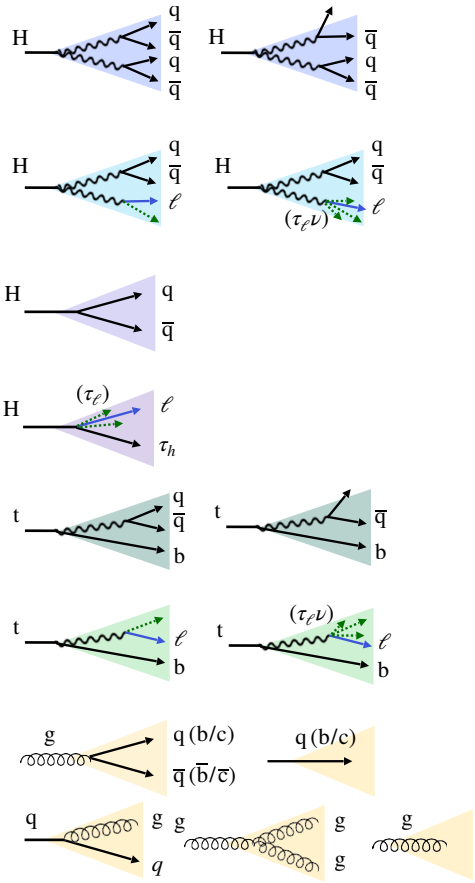


Figure 2. Full suite of AK8 jet topologies considered for the ParT multiclass classification task. Jet types are first categorized by the number of quarks and leptons in the final state, and then further separated by flavor, as shown in the table on the left. The symbols τ_e, τ_μ, and τ_h refer to τ lepton decays to electrons, muons, and hadrons, respectively. The total number of subclasses for each process, therefore, is given by the tensor product ($\otimes$) between the different final states and flavors. Diagrams illustrating the corresponding jet topologies, which are not exhaustive, are shown on the right.

for the H → WW topologies. Namely, if m_W were to remain fixed to its SM value, three distinct kinematic phases would be present in the training samples for the H → WW topology as a function of m_H: 1) two off-shell W bosons for $m_H \lesssim m_W$; 2) one off-shell and one on-shell W boson for $m_W \lesssim m_H \lesssim 2m_W$; and 3) two on-shell W bosons for $m_H \gtrsim 2m_W$. This variation in the jet kinematics was found to harm the model performance on the SM H → WW* topology, as well as to introduce biases in the performance with respect to the jet mass. To address this, training samples are generated with varying m_W as well, as described in section 4, ensuring ParT is optimized for the SM H → WW* on-shell plus off-shell topology and improving its mass decorrelation.

To further improve decorrelation, we ensure training classes share similar mass distributions by sampling uniformly in the two-dimensional (2D) m_{SD} and $\ln(p_T/\text{GeV})$ per class, as in ref. [11]. The 2D sampling weights are derived in 10 GeV bins of m_{SD} between 20

JHEP10(2026)167

and 260 GeV and 11 bins in p_T uniformly distributed in logarithmic scale between 200 and 2500 GeV, ensuring a uniform distribution in m_{SD} and $\ln(p_T/\text{GeV})$.

Additionally, jets from each class are sampled during the training according to the relative weights in table 3 to balance the class distributions. Each of the four major processes: $H \to WW^*$, $H \to$ 2-pronged, t, and QCD jets are weighted equally; i.e., the weights in each row in table 3 sum to unity. Within each process, the classes are weighted according to the SM branching fractions, except for $H \to$ 2-pronged jets, where the $b\bar{b}$, $c\bar{c}$, $s\bar{s}$, and $q\bar{q}$ classes are all weighted equally to avoid the $b\bar{b}$ final state dominating because of its significantly higher branching fraction. We find that moderate variations in the weighting scheme (i.e., within approximately one order of magnitude) have little impact on the network performance; in particular, networks trained with different weight configurations can be made equivalent by rescaling the output probability scores. The choice of weights is therefore mainly driven by technical considerations for class balance.

The training is performed using the Weaver framework [107], a DL toolkit based on the PyTorch [108] Python library, on three Nvidia GTX 3090 GPUs in parallel. The total data set comprises 52.4 million jets, with 80% reserved for training and 20% for validation, and we use a batch size of 512 jets. As shown in ref. [32], training a high-performance transformer-based jet tagging model typically requires tens of millions of jets, preferably approaching 100 million. The data set size used in this work is sufficient to achieve strong performance while remaining computationally tractable. Rather than one pass of the entire data set defining an epoch, we define one epoch as processing 15,000 batches or 7.68 million jets (sampled from 80% of the data set) for training and 1000 batches or 0.512 million jets (sampled from the remaining 20%) for validation, continuously iterating through the data set. The model is trained over 50 epochs. A model snapshot is saved at the end of each epoch, and the model with the lowest hybrid loss on the evaluation set is selected as the final model. The Lookahead optimizer [109], paired with RAdam [110] as the inner optimizer, is used for training. The initial learning rate is set to 5×10^{-3}, remaining constant for the first 70% of iterations before decaying exponentially at the start of each subsequent epoch, and reaching 1% of the initial value by the final epoch. Figure 3 presents the loss curves during the training for the training and validation data sets, separated into the classification (cross-entropy) and regression (log-cosh) terms. No evidence of overfitting is observed.

5.3 Performance of jet mass reconstruction

The performance of the ParT algorithm in reconstructing the jet mass is shown in figure 4 for jets originating from four different processes: $H \to b\bar{b}$, $H \to WW^* \to 4q$, $t \to bq\bar{q}$, and QCD, for the SM values of $m_H = 125$ GeV, $m_t = 172.5$ GeV, and $m_W = 80.4$ GeV. An offline selection of $p_T > 400$ GeV and $|\eta| < 2.4$ is applied to the AK8 jets, where the p_T selection is more stringent to ensure that the decay products are fully contained within the AK8 jet cone and the full jet mass distribution can be shown up to 250 GeV. The reconstructed jet mass distributions using the SD and ParticleNet algorithms are also shown for comparison. The ParticleNet mass regression algorithm was trained using $H \to b\bar{b}$, $H \to c\bar{c}$, $H \to q\bar{q}$, and QCD jets, with m_H ranging from 15 to 250 GeV [12]. The mass of the resonance peaks m_{peak} is extracted by locating the maximum of a Gaussian kernel-smoothed mass distribution

JHEP10(2026)167

Process	$H \to WW^*$							$H \to$ 2-pronged							$t \to bW$							QCD
Final state	qqqq	qqq	eνqq	$\mu\nu$qq	$\tau_e\nu$qq	$\tau_\mu\nu$qq	$\tau_h\nu$qq	$b\bar{b}$	$c\bar{c}$	$s\bar{s}$	$q\bar{q}$	$\tau_e\tau_h$	$\tau_\mu\tau_h$	$\tau_h\tau_h$	$bq\bar{q}$	bq	beν	b$\mu\nu$	b$\tau_e\nu$	b$\tau_\mu\nu$	b$\tau_h\nu$	All
Weight	0.32	0.08	0.2	0.2	0.03	0.03	0.14	0.16	0.16	0.16	0.16	0.08	0.08	0.2	0.32	0.08	0.2	0.2	0.03	0.03	0.14	1

Table 3. Relative weights of each of the classes used for training the ParT model. Each of the four major processes: $H \to WW^*$, $H \to$ 2-pronged, $t \to bW$, and QCD jets, are weighted equally and have one row dedicated to them each.

JHEP10(2026)167

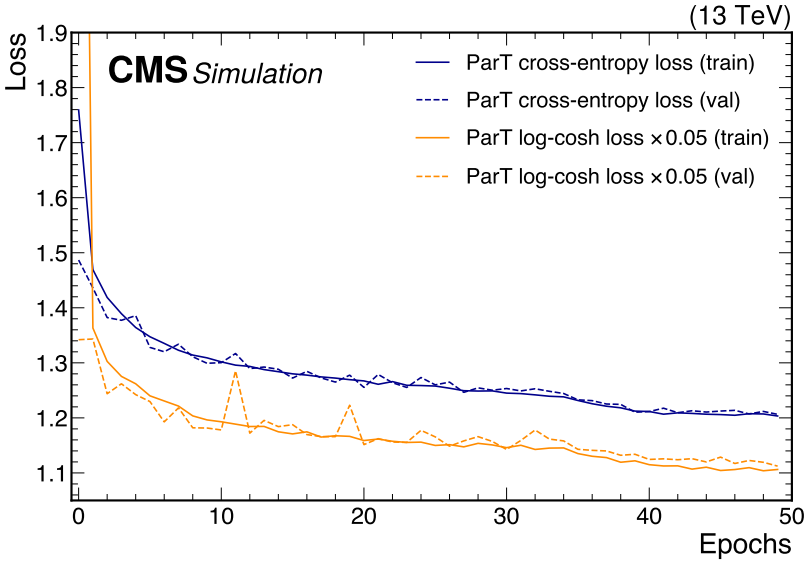


Figure 3. Evolution of the loss function values for the ParT model on the training and validation data sets over training epochs, shown separately for the classification (cross-entropy) and regression (log-cosh) terms.

obtained from each histogram, with the mass resolution quantified by the full width at half maximum (FWHM) of the peak. Both quantities are shown in the legend of figure 4 for each algorithm and resonant process.

We observe improved mass resolution from both ParticleNet and ParT with respect to m_{SD} for the two-pronged $\mathrm{H} \to \mathrm{b\bar{b}}$ decay, while ParT in particular is the most performant for the higher-pronged $\mathrm{H} \to \mathrm{WW}^* \to 4\mathrm{q}$ and $\mathrm{t} \to \mathrm{bq\bar{q}}$ decays. This is expected because the SD algorithm was not specifically optimized for these 4- and 3-pronged decays, and ParticleNet was also not trained on these decays. One feature of the SD algorithm shown in figure 4, using the CMS parameters described in section 3, is a relatively strong removal of PF candidates from the jet. This yields an m_{SD} value close to 0 GeV for a significant fraction of H and t jets, and a large tail in the m_{SD} distribution below the true mass. Despite this, the resolution and scale of m_{SD} have been verified and calibrated with 3-pronged t jets in Run 2 and Run 3 data [111, 112]. We observe a slight bias towards a higher predicted reconstructed mass for H and t jets than the true values from both ParticleNet and ParT, which we attribute to the presence of high-mass jets in the training sample. Finally, we observe smoothly falling distributions for QCD jets for all three algorithms.

6 Performance and calibration of $\mathrm{H} \to \mathrm{WW}^*$ tagging

6.1 Performance

To evaluate the performance of the $\mathrm{H} \to \mathrm{WW}^*$ tagging, we use a single discriminant focusing on distinguishing hadronic $\mathrm{H} \to \mathrm{WW}^*$ jets from t and QCD multijet jets, defined as

$$T_{\mathrm{HWW}} = \frac{P_{\mathrm{HWW4q}} + P_{\mathrm{HWW3q}}}{P_{\mathrm{QCD}} + P_{\mathrm{top}} + P_{\mathrm{HWW4q}} + P_{\mathrm{HWW3q}}}, \tag{6.1}$$

JHEP10(2026)167

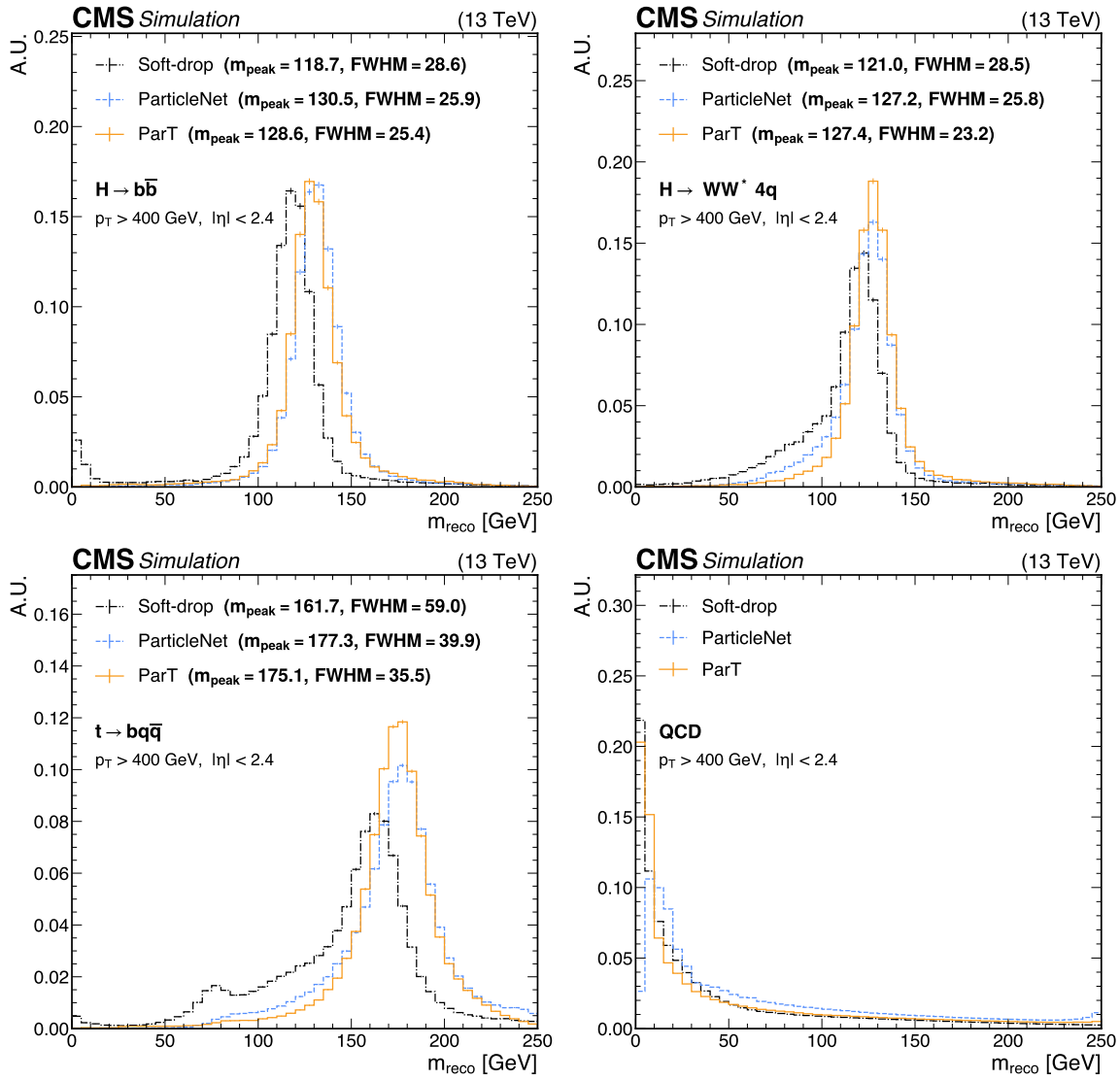


Figure 4. Comparison of jet mass reconstruction (m_{reco}) using the SD, ParticleNet, and ParT algorithms, for $\mathrm{H} \to \mathrm{b\bar{b}}$ (upper left), $\mathrm{H} \to \mathrm{WW}^* \to 4\mathrm{q}$ (upper right), $\mathrm{t} \to \mathrm{bq\bar{q}}$ (lower left), and QCD (lower right) jets with the SM values of m_{H} and m_{t}. An offline selection of $p_{\mathrm{T}} > 400\,\mathrm{GeV}$ and $|\eta| < 2.4$ is applied to the AK8 jets. Statistical uncertainties in the bin yields originating from the limited number of simulated events are represented by vertical error bars. The mass at the peak (m_{peak}) for each algorithm, calculated using Gaussian kernel density estimation, and the mass resolution, quantified by the FWHM of the resonance peak, are shown as well for H and t jets.

JHEP10(2026)167

where P_{HWW4q}, P_{HWW3q}, P_{top}, and P_{QCD} are the sum of the predicted probabilities of their respective subcategories.

The performance of the tagger using this discriminant in differentiating between SM $\mathrm{H} \to \mathrm{WW}^*$ "signal" and QCD and t background jets is shown in the receiver operating characteristic curves in figure 5, where signal and background efficiencies are defined as the fraction of signal and background jets passing a given discriminant threshold. The curves are provided for several ranges of jet p_{T}. For the H and t jets, we use only the AK8 jets that lie within $\Delta R < 0.8$ of the generator-level H or t, respectively, while for QCD we select the jet with the highest p_{T} in the event. An offline selection of $p_{\mathrm{T}} > 200\,\mathrm{GeV}$, $m_{\mathrm{SD}} > 30\,\mathrm{GeV}$, and $|\eta| < 2.4$ is applied to all jets.

We compare our model with the mass-decorrelated DeepAK8-MD algorithm [4], which was previously state-of-the-art in CMS for $\mathrm{H} \to \mathrm{WW}^*$ jet identification. Unlike the ParT algorithm, which respects inductive biases of jets such as permutation invariance and heterogeneity of the jet constituents, the DeepAK8-MD algorithm represents jets as lists of PF candidates and SVs and uses a convolutional neural network architecture inspired by ResNet [113] for classification. The total number of parameters in the DeepAK8-MD model is about 500,000, and the mass decorrelation is achieved with an adversarial training approach [78]. The mass-decorrelated ParticleNet-MD algorithm was only trained to distinguish between $\mathrm{H} \to \mathrm{b\bar{b}}$, $\mathrm{H} \to \mathrm{c\bar{c}}$, $\mathrm{H} \to \mathrm{q\bar{q}}$, and QCD jets [11], so it cannot be used as a baseline for $\mathrm{H} \to \mathrm{WW}^*$ jet identification.

The DeepAK8-MD algorithm was trained on approximately 40 million jets to distinguish among jets originating from $\mathrm{H} \to 4\mathrm{q}$ (output P_{H4q}), $\mathrm{W} \to \mathrm{q\bar{q}}$ (P_{Wqq}), $\mathrm{t} \to \mathrm{bq\bar{q}}$ (P_{top}) decays, and others. A discriminant targeting $\mathrm{H} \to 4\mathrm{q}$ and $\mathrm{W} \to \mathrm{q\bar{q}}$ jets, while vetoing QCD jets, can be constructed from its outputs, as in refs. [21, 22]. To further improve the suppression of the $\mathrm{t\bar{t}}$ background, the DeepAK8-MD discriminant can be extended to veto both QCD and $\mathrm{t} \to \mathrm{bq\bar{q}}$ jets. The resulting discriminant, referred to as the DeepAK8-MD score, is defined as

$$\text{DeepAK8-MD score} = \frac{P_{\mathrm{Wqq}} + P_{\mathrm{H4q}}}{P_{\mathrm{QCD}} + P_{\mathrm{top}} + P_{\mathrm{Wqq}} + P_{\mathrm{H4q}}}. \tag{6.2}$$

The performance of this discriminant is shown in figure 5 as well. We observe up to ten times stronger QCD jet rejection for the same signal efficiencies using ParT with respect to the DeepAK8-MD score, and up to eight times stronger t jet rejection. Thus, through the architectural and training advancements described in this paper, ParT significantly outperforms DeepAK8-MD.

We additionally evaluate the performance of ParT in identifying BSM scalar resonances Y decaying to SM W bosons, shown in figure 6. We observe that, despite being optimized exclusively for the SM $m_{\mathrm{W}}/m_{\mathrm{H}}$ ratio, ParT performs similarly for a small range of m_{Y} away from the SM m_{H}; however, there is some performance degradation for $m_{\mathrm{Y}} = 250\,\mathrm{GeV}$, at the boundary of the training mass range. This suggests that ParT can be used to search for general BSM $\mathrm{Y} \to \mathrm{WW} \to 4\mathrm{q}$ signatures for $m_{\mathrm{Y}} < 250\,\mathrm{GeV}$ [114]. The 15–250 GeV range of resonance masses in the training samples was primarily chosen to decorrelate the tagger response from the jet mass for resonances near the SM Higgs boson mass. For $m_{\mathrm{Y}} > 250\,\mathrm{GeV}$, ParT is therefore applied outside the mass range covered in training. The degradation

JHEP10(2026)167

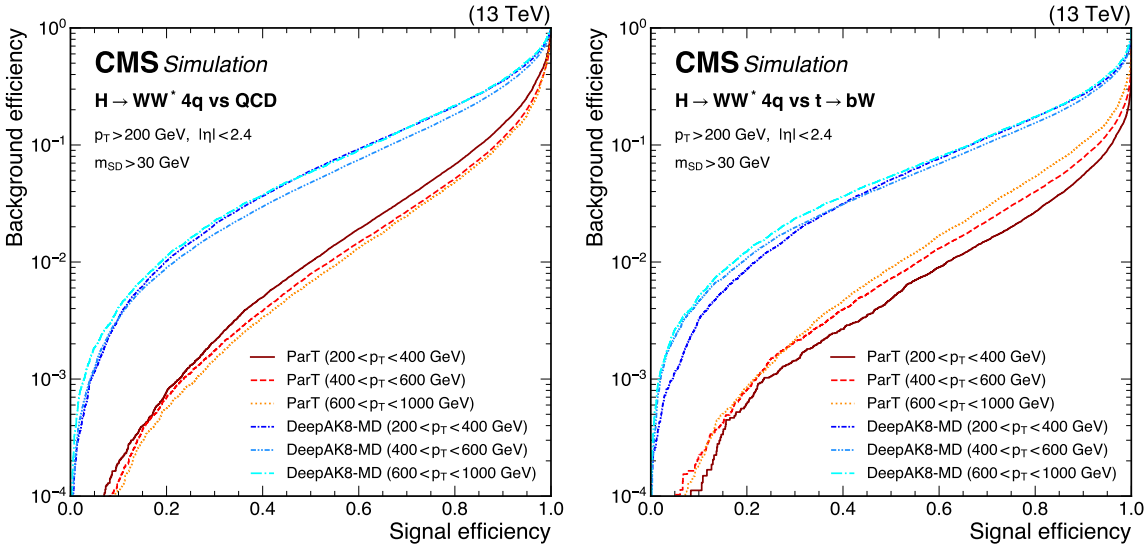


Figure 5. Receiver operating characteristic curves for $H \to WW^*$ signal jets, with the SM values of m_H and m_t, versus background jets from simulated QCD multijet (left) and $t\bar{t}$ events (right), for the ParT T_{HWW} and the DeepAK8-MD scores in the p_T ranges 200–400, 400–600, and 600–1000 GeV. An offline selection of $p_T > 200$ GeV and $|\eta| < 2.4$ is applied to the AK8 jets. Signal jets are required to contain all four generator-level quarks from the W boson decays within $\Delta R(\text{jet}, q) < 0.8$.

seen at the boundary continues: in the $X \to HY$ search of ref. [114], the selection efficiency for signal jets with m_Y above this range is lower by about a factor of three than for those with m_Y within it. Extending the training mass range would benefit searches targeting heavier resonances, and is left for future work. Finally, figure 7 shows the confusion matrix, with each row indicating the fraction of jets per category classified as the column category by ParT. We observe generally strong agreement between the true and predicted classes, with higher misclassification rates within subcategories with similar final states, such as $H \to WW^* \to \tau_e \nu qq$ and $H \to WW^* \to e\nu qq$, as expected.

6.2 Mass decorrelation

In many analyses, it is desirable for the tagger to be decorrelated with the jet mass, as this allows for the use of sideband regions in the jet mass distribution to constrain backgrounds and reduce systematic uncertainties [47]. The decorrelation of ParT's outputs with the jet mass is examined in figure 8 for jets in simulated QCD multijet events. Figure 8 also presents the performance of the DeepAK8-MD discriminant for comparison, which uses an adversarial training strategy for mass decorrelation. To quantify the degree of mass decorrelation, we consider the Jensen-Shannon distance (JSD) [115] using base 2, a symmetrized variant of the Kullback-Leibler divergence [116], between the m_{SD} distributions with and without ParT and DeepAK8-MD selections. The JSD quantifies the difference between the two distributions and is bounded between 0 and 1, with a lower value indicating better agreement and, hence, better decorrelation. It is reported in figure 9 for a range of different tagger selection efficiencies and jet p_T bins.

JHEP10(2026)167

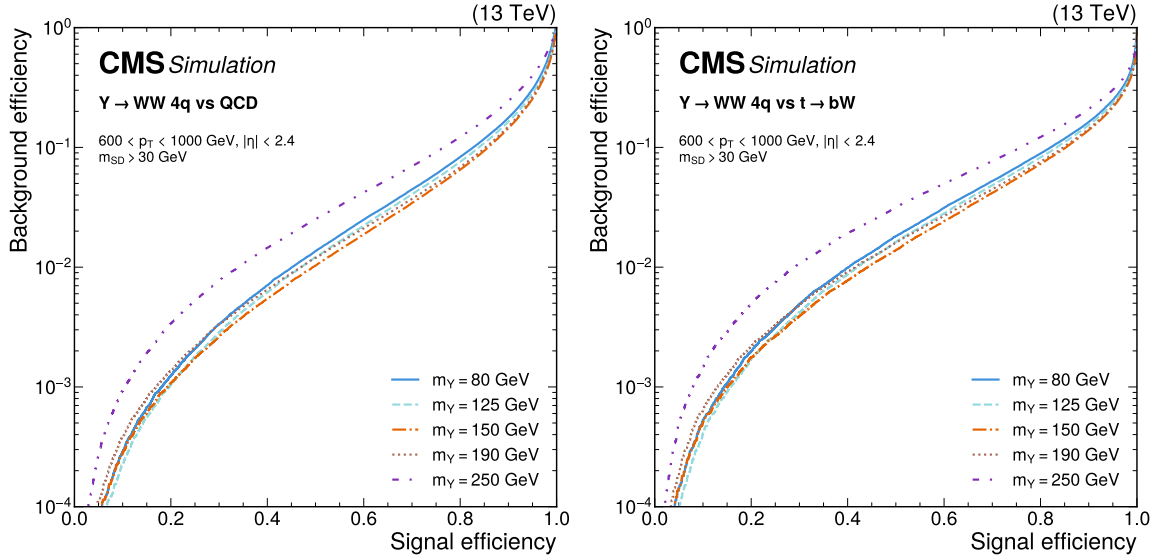


Figure 6. Receiver operating characteristic curves for $\mathrm{Y} \to \mathrm{WW}$ signal jets, with varying m_{Y} and SM m_{W}, versus background jets from simulated QCD multijet (left) and $\mathrm{t\bar{t}}$ events (right), for the ParT T_{HWW} score. An offline selection of $600 < p_{\mathrm{T}} < 1000\,\mathrm{GeV}$, $|\eta| < 2.4$, and $m_{\mathrm{SD}} > 30\,\mathrm{GeV}$ is applied to the AK8 jets.

We observe that the m_{SD} distributions remain generally consistent within statistical uncertainties across increasingly tighter selections on the ParT T_{HWW} discriminant; however, there is some evidence of discrepancies in the tails, motivating an increase of the training mass range. This will be the subject of future work. Furthermore, by using samples of varying resonance masses for ParT rather than the adversarial approach of DeepAK8-MD, we are able to employ a simpler loss function and obviate the challenge of training a model with competing objectives; thus, we observe consistently lower JSD values for ParT across a range of selection efficiencies and jet p_{T}.

6.3 Calibration using the Lund jet plane

Jet identification algorithms are typically calibrated using a similar but more abundant SM process as a proxy for the signal process. For example, for boosted $\mathrm{H} \to \mathrm{b\bar{b}}$ calibration, the CMS experiment has used jets produced through Z boson decays to $\mathrm{b\bar{b}}$ and through gluon splitting to $\mathrm{b\bar{b}}$ to measure data versus signal simulation disagreement in the tagger score modeling [117]. However, for $\mathrm{H} \to \mathrm{WW}^* \to 4\mathrm{q}$ jets, it is difficult to define such a high-purity data sample of four-pronged jets. Instead, we use a novel method that measures data versus simulation differences in the per-subjet radiation pattern based on densities of their primary LJPs [48], as introduced in ref. [49].

The primary LJP of a jet represents each successive hardest splitting in the 2D $(\ln(1/\Delta), \ln(k_{\mathrm{T}}/\mathrm{GeV}))$ plane, where Δ and k_{T} are the same quantities defined in section 5.1, evaluated here for the emitting and emitted particles of each splitting. As discussed in ref. [48], the primary LJP captures important information about the substructure of the jet. The ratio of the densities of primary LJPs of jets from data and simulation are measured in ref. [49]

JHEP10(2026)167

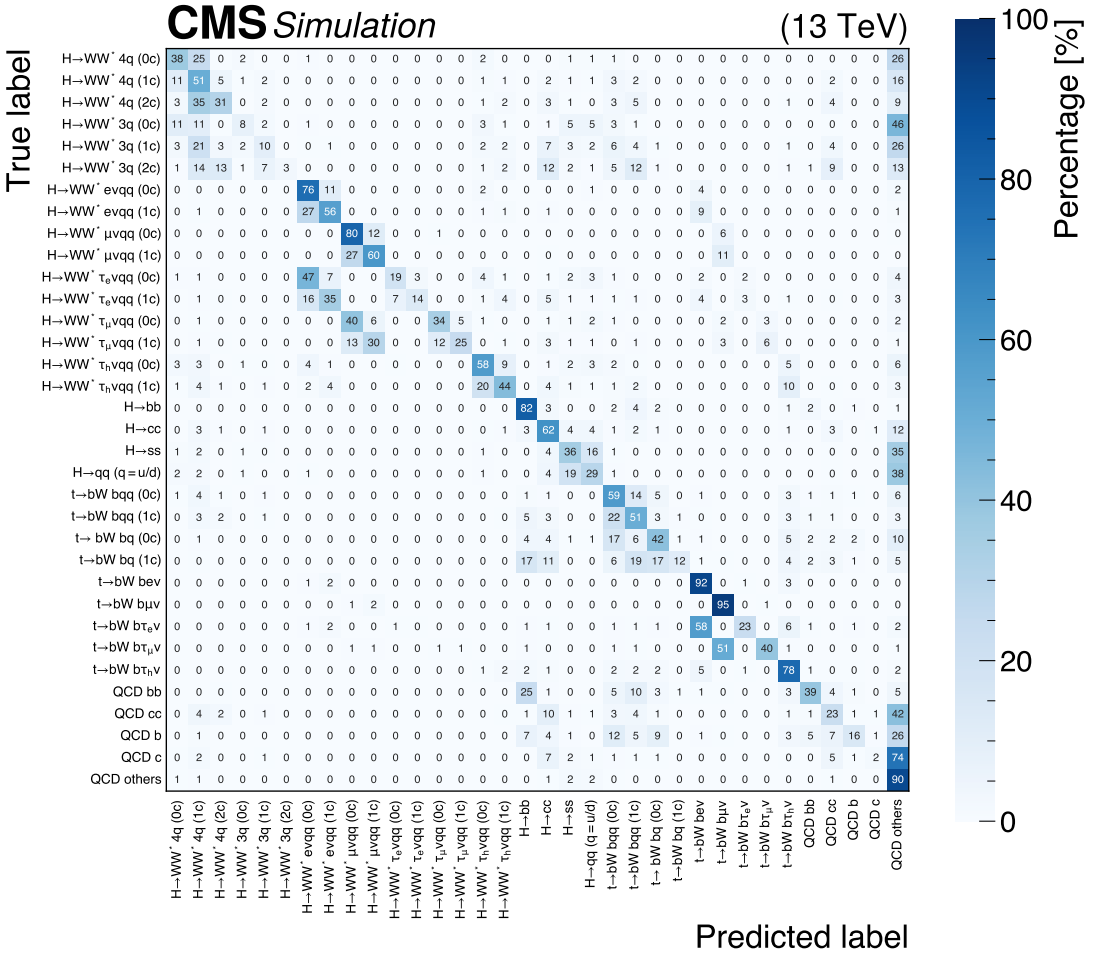


Figure 7. Confusion matrix with each row indicating the fraction of jets per category classified as the column category by ParT. An offline selection of $p_T > 200\,\text{GeV}$ and $|\eta| < 2.4$ is applied to the AK8 jets.

per subjet in merged two-pronged jets originating from W bosons, clustered with the k_T algorithm to two exclusive jets, and binned in subjet p_T.

To measure a correction for the signal efficiency, first, a data-to-simulation relative weight per event is derived for the signal using the primary LJP splittings for each subjet in the $H \to WW^*$ jet, following the procedure described in ref. [49]. Each $H \to WW^*$ jet is categorized as either two-, three-, or four-pronged based on the number of quarks within the jet radius, using information from the event generator, and is then reclustered into the corresponding number of subjets. The relative event weight is defined as the product, taken over all subjets in each splitting, of the data-to-simulation density ratios of primary LJPs,

JHEP10(2026)167

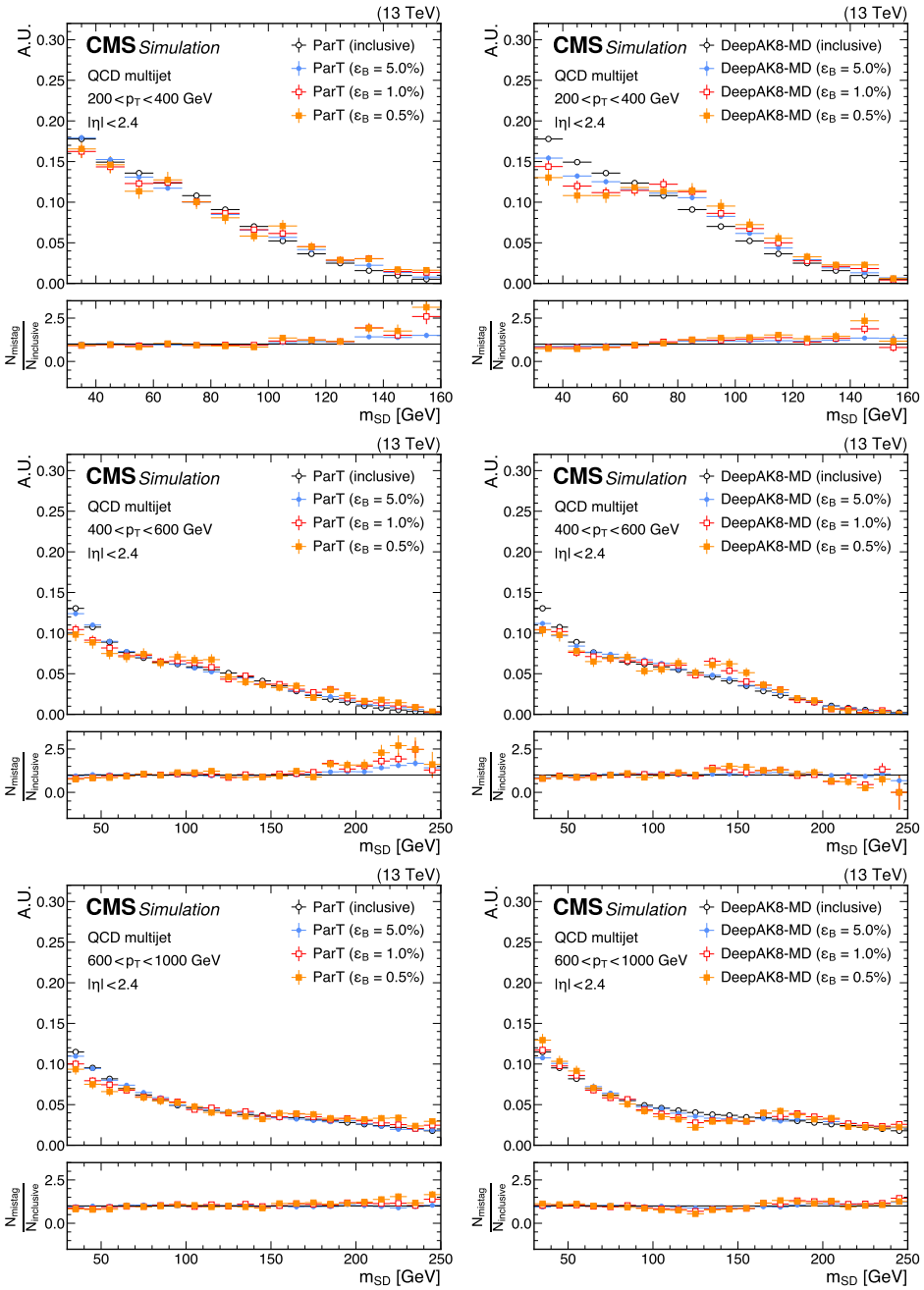


Figure 8. Distributions of m_{SD} for jets from QCD multijet events, in the p_{T} ranges 200–400 GeV (upper), 400–600 GeV (middle) and 600–1000 GeV (lower), after no selections ("inclusive") on the ParT T_{HWW} score (left) and the DeepAK8-MD score (right) as well as selections corresponding to QCD jet selection efficiencies (ϵ_B) of 5.0%, 1.0%, and 0.5%. The error bars represent the statistical uncertainties originating from the limited number of simulated events. The lower panels display the ratio of the normalized m_{SD} distributions for the different selection efficiencies (N_{mistag}) to the normalized inclusive m_{SD} distribution ($N_{\mathrm{inclusive}}$). An offline selection of $p_{\mathrm{T}} > 400\,\mathrm{GeV}$, $|\eta| < 2.4$, and $m_{\mathrm{SD}} > 30\,\mathrm{GeV}$ is applied to the AK8 jets.

JHEP10(2026)167

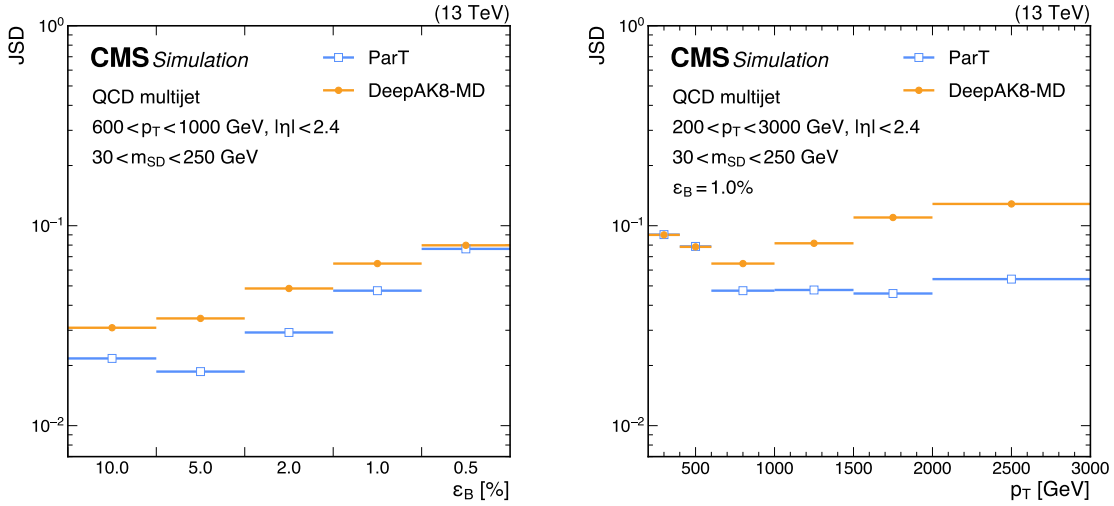


Figure 9. The Jensen-Shannon distance (JSD) using base 2 between the m_{SD} distribution of jets from QCD multijet events with and without a selection on the ParT and DeepAK8-MD tagger scores. On the left, the JSD is plotted for tagger selections corresponding to different QCD jet selection efficiencies (ϵ_{B}), with an offline selection of $600 < p_{\mathrm{T}} < 1000\,\mathrm{GeV}$, $|\eta| < 2.4$, and $30 < m_{\mathrm{SD}} < 250\,\mathrm{GeV}$ applied to the jets. On the right, the JSD is plotted for different jet p_{T} bins, at a fixed ϵ_{B} of 1%.

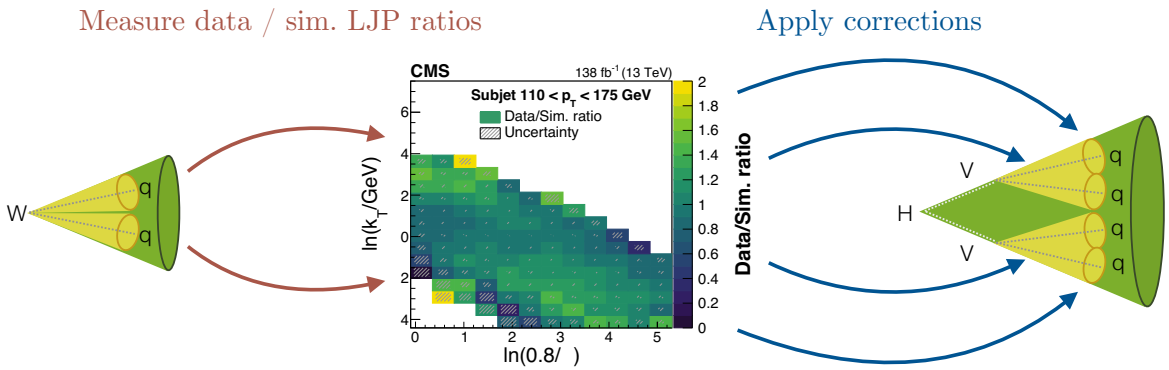


Figure 10. Schematic of the LJP calibration method for $\mathrm{H} \to \mathrm{WW}^*$ tagging. Ratios of primary LJP densities in data and simulation are first measured per subjet in merged two-pronged W jets, with an example of such a ratio reproduced from ref. [49]. These are then used to derive correction factors for $\mathrm{H} \to \mathrm{WW}^*$ signal jets per prong.

parameterized by k_{T}, Δ, and the subjet p_{T}. Systematic uncertainties related to the validity of this procedure and the quark-subjet correspondence are discussed below. The final event weights are then either applied to the simulated signal events, as in the top quark validation study shown in figure 11 below, or used to derive a single data-to-simulation scale factor (SF), defined as the ratio of the signal yield with and without the event weights, as in the HH search in section 7. A schematic of the overall calibration procedure is shown in figure 10.

Uncertainties from the correction procedure are propagated as systematic uncertainties in the SF. The following sources are considered, as described in detail in ref. [49]: 1) statistical

JHEP10(2026)167

Region	Process	SF	Uncertainty components (fractional)					
			Ratio stat.	Ratio syst.	p_T extrap.	# prongs	Unclust. prongs	Dist.
ggF	SM ggF HH	$0.91^{+0.19}_{-0.13}$	0.02	0.08	0.00	0.03	$^{+0.17}_{-0.08}$	$^{+0.09}_{-0.08}$
	SM VBF HH	$0.94^{+0.22}_{-0.18}$	0.02	0.15	0.00	0.01	$^{+0.16}_{-0.07}$	$^{+0.07}_{-0.08}$
	VBF HH ($\kappa_{2V} = 0$)	$0.99^{+0.17}_{-0.08}$	0.02	0.02	0.01	0.02	$^{+0.17}_{-0.07}$	$^{+0.02}_{-0.00}$
	VBF HH ($\kappa_{2V} = 2$)	$1.00^{+0.18}_{-0.07}$	0.02	0.01	0.01	0.02	$^{+0.17}_{-0.07}$	$^{+0.02}_{-0.00}$
VBF	SM ggF HH	$0.83^{+0.22}_{-0.15}$	0.03	0.13	0.01	0.04	$^{+0.20}_{-0.09}$	$^{+0.09}_{-0.07}$
	SM VBF HH	$0.91^{+0.21}_{-0.19}$	0.02	0.18	0.00	0.02	$^{+0.12}_{-0.05}$	$^{+0.07}_{-0.07}$
	VBF HH ($\kappa_{2V} = 0$)	$0.88^{+0.14}_{-0.09}$	0.02	0.07	0.01	0.02	$^{+0.14}_{-0.06}$	$^{+0.03}_{-0.01}$
	VBF HH ($\kappa_{2V} = 2$)	$0.89^{+0.14}_{-0.08}$	0.02	0.06	0.01	0.02	$^{+0.13}_{-0.06}$	$^{+0.03}_{-0.01}$

Table 4. Signal efficiency SFs and uncertainties for the BDT selections on the ParT $H \to WW^*$ tagging outputs in the $HH \to b\bar{b}WW^*$ search, measured using the LJP calibration method for different HH signals and analysis regions. Both the total combined uncertainty and the components defined in the text are shown.

uncertainties in the derived LJP ratio from the limited number of data events in the W boson enriched sample ("ratio stat."); 2) systematic uncertainties in the ratio because of possible simulation mismodeling ("ratio syst."), estimated using "tag and probe" measurements; 3) uncertainties in the extrapolation of the SF to high p_T subjets ("p_T extrap."); 4) uncertainties in the true number of prongs inside the $H \to WW^*$ jet ("# prongs"); 5) whether there exists a correct, one-to-one correspondence between the reclustered subjets and $H \to WW^*$ daughter quarks ("unclust. prongs"); and 6) differences between the LJP densities of the W boson jets used for the correction and the $H \to WW^*$ signal jets ("distortion"). The impacts of these uncertainties for different HH signals are quantified in table 4. Generally, the uncertainty in the unclustered prongs is dominant, followed by systematic uncertainties in the LJP ratios and the distortion uncertainties.

6.4 Validation on jets from boosted top quark decays

The LJP calibration method is validated for ParT on jets from decays of boosted top quark candidates. We define a semileptonic boosted $t\bar{t}$ enriched data sample, tagging a leptonically decaying top quark ($t \to bW \to b\mu\nu$), and probing an opposite-side high-p_T AK8 jet representing the hadronically decaying top quark. The event selection follows that of the control region in ref. [49], comprising muon triggers and offline selections for a b-tagged AK4 jet, a leptonically decaying W boson — based on the presence of a muon and p_T^{miss} — and a high-p_T AK8 jet with a mass close to m_t. Jets from simulated $t\bar{t}$ samples are categorized using generator-level particles as either: "t-matched" — with all three daughter quarks lying within the jet; "W-matched" — with only the W daughter quarks inside the jet; or "t- and W-unmatched" — neither of these two cases. Only the t-matched jets are reweighted with the LJP ratios, as they are expected to be the most similar to the $H \to WW^*$ signal jets and, indeed, dominate the high-scoring bins in figure 11.

JHEP10(2026)167

We consider the T_{HWW} discriminant from eq. (6.1), excluding P_{top} from the denominator to retain top quark events in the high tagger score bins:

$$T_{\mathrm{HWW}}^{\text{No top}} = \frac{P_{\mathrm{HWW4q}} + P_{\mathrm{HWW3q}}}{P_{\mathrm{QCD}} + P_{\mathrm{HWW4q}} + P_{\mathrm{HWW3q}}}. \tag{6.3}$$

The $T_{\mathrm{HWW}}^{\text{No top}}$ distributions from the 2017 data sets before and after LJP-reweighting of the events with matched top quark jets are shown in figure 11 (left). The combined uncertainties per bin are also shown in the distributions and data versus simulation ratios. We observe an overall improvement in the agreement between data and simulation, with the χ^2 test statistic value decreasing from 20.7 to 16.6 for 20 degrees of freedom, corresponding to an increase in the two-tailed p-value from 0.415 to 0.679. Importantly, the data and simulation yields are all consistent within statistical and systematic uncertainties in these bins. We also show the effect of LJP calibration of the DeepAK8-MD discriminant in figure 11 (right), defined similarly as in eq. (6.2), excluding P_{top} from the denominator:

$$\text{DeepAK8-MD score (No top)} = \frac{P_{\mathrm{Wqq}} + P_{\mathrm{H4q}}}{P_{\mathrm{QCD}} + P_{\mathrm{Wqq}} + P_{\mathrm{H4q}}}. \tag{6.4}$$

We observe a larger improvement in the agreement between data and simulation; however, overall, the agreement is worse than that of ParT. The calibration is also performed in the 2016 and 2018 data sets, with similar corrections and improvements in the agreement between data and simulation.

7 Impact on measuring HH $\to$ b$\bar{\mathrm{b}}$WW* production properties

Targeting boosted H $\to$ WW* production is motivated by a variety of BSM scenarios, including the production of heavy resonance decays of the form X $\to$ HY, where X and Y are new scalar resonances with H $\to$ b$\bar{\mathrm{b}}$ and Y $\to$ VV $\to$ 4q [114], and measurements of Higgs boson couplings through the production of Higgs boson pairs [50]. One property of the Higgs boson that is particularly challenging to measure is its quartic HHVV coupling. Deviations to this coupling can significantly enhance VBF HH, particularly at high HH invariant mass, which is why recent searches for boosted HH $\to$ b$\bar{\mathrm{b}}$b$\bar{\mathrm{b}}$ have been successful in constraining this coupling [16, 17]. This motivates further exploration of boosted HH production, particularly for the first time in the all-hadronic b$\bar{\mathrm{b}}$WW channel [50], which represents the largest branching fraction of HH decays after b$\bar{\mathrm{b}}$b$\bar{\mathrm{b}}$. However, such a search necessitates powerful classification algorithms for both H $\to$ b$\bar{\mathrm{b}}$ and WW* to discriminate against the dominant QCD multijet background. This section summarizes the use of ParT in the first all-hadronic HH $\to$ b$\bar{\mathrm{b}}$WW* search; a more detailed description of the search can be found in section 4.4.2 of ref. [50].

The primary physics objects considered in the search are two large-radius (AK8) jets, each representing one of the two Higgs bosons, which are tagged as H $\to$ b$\bar{\mathrm{b}}$ candidates and H $\to$ WW* candidates using DL algorithms. Offline selections are defined using a selection on the H $\to$ b$\bar{\mathrm{b}}$ tagging score of the b$\bar{\mathrm{b}}$ candidate jet, and multivariate selections using a boosted decision tree (BDT) on the ParT scores of the WW* candidate, along with kinematic variables, targeting the ggF and VBF production modes. Working points for the BDT are

JHEP10(2026)167

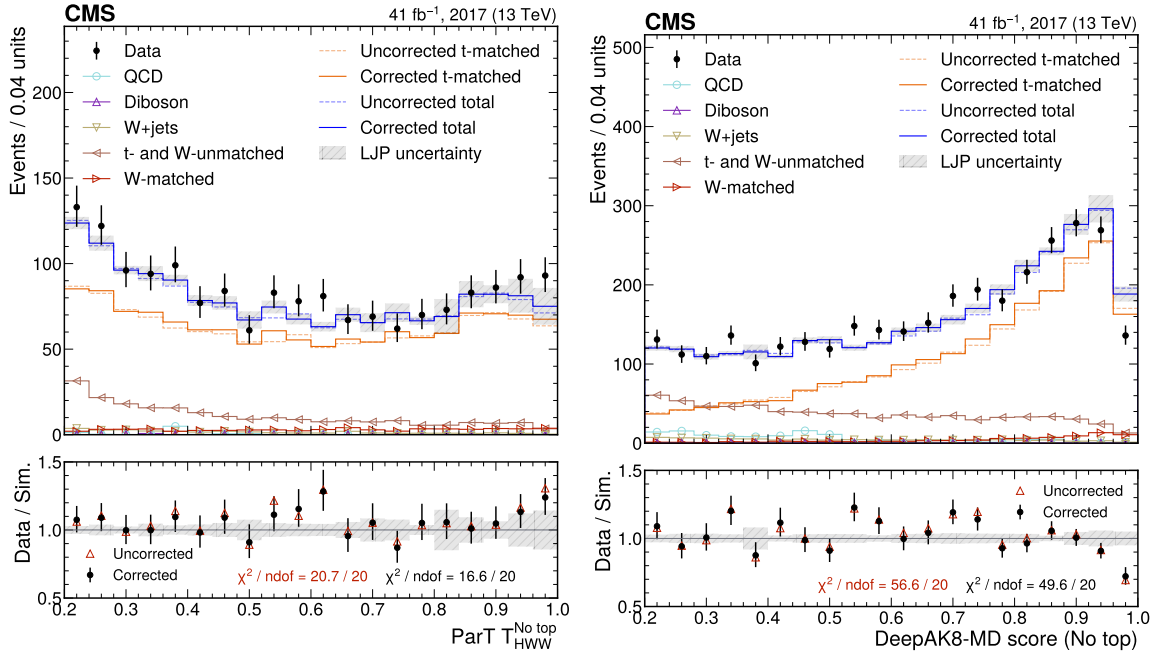


Figure 11. Distributions of the ParT $T_{HWW}^{No\ top}$ (left) and DeepAK8-MD (No top) (right) discriminants with and without the LJP corrections for t-matched jets for data and individual simulated processes in the upper panels, and data versus simulation ratios in the lower panels. The combined uncertainties from LJP-based SFs per bin are shown in shaded gray, and the statistical uncertainty in the number of data events per bin is represented by vertical error bars in the upper and lower panels. The χ^2 test statistic values between data and simulation, normalized to the number of degrees of freedom (ndof), are also shown for both discriminants with and without LJP corrections.

optimized for expected limits for ggF and VBF HH cross sections, with signal (background) efficiencies of 7% (≈0.01%) and 20% (≈0.003%), respectively. As the ParT scores of the WW* candidate rank highest in feature importance among all the inputs to the BDT, the ParT algorithm is critical to achieving this level of signal-to-background discrimination.

Several sources of theoretical and experimental systematic uncertainties are considered in the signal and background modeling in the signal regions. Overall, the dominant uncertainty in the HH signal strength is the statistical uncertainty in the QCD multijet background estimation, driven by the limited data sample size in the signal region, with an impact on the best fit signal strength of 50% relative to the overall uncertainty. The next largest source of uncertainty is in the signal efficiency of the BDT selections on the ParT H → WW* tagging outputs, measured using the LJP method. A summary of the calculated SFs and uncertainties for different HH signals and signal regions is provided in table 4, where the overall uncertainty ranges between 15 and 25%, and has a relative impact of 23% on the best fit signal strength. Among all the channels included in the CMS HH combination, the all-hadronic $b\bar{b}WW$ channel provides the second most stringent constraint on the κ_{2V} coupling of $[-0.04, 2.05]$ at 68% confidence level (CL), after the boosted $b\bar{b}b\bar{b}$ channel ($[0.62, 1.41]$ at 68% CL) [50].

JHEP10(2026)167

8 Summary

The particle transformer (ParT) deep neural network for classifying a wide variety of jets from decays of Lorentz-boosted resonances has been presented. In particular, ParT enables effective identification of all-hadronic Higgs boson to W boson ($H \to WW^* \to 4q$) decays by the CMS experiment for the first time. A novel training strategy is used to address challenges pertaining to $H \to WW^*$ classification, through which ParT achieves >50% $H \to WW^* \to 4q$ selection efficiency with a multijet background efficiency of 1%, while maintaining decorrelation with the jet mass. The performance is calibrated on data using the primary Lund jet planes of individual subjets, with data-to-simulation scale factors measured in the 0.9–1.0 range, and relative uncertainties between 7 and 23%. The ParT algorithm represents a significant advancement in the identification capabilities of multiprong jets from highly boosted resonances in CMS, illustrated by the first search for boosted Higgs boson pair production in the all-hadronic $b\bar{b}WW$ channel.

Acknowledgments

We congratulate our colleagues in the CERN accelerator departments for the excellent performance of the LHC and thank the technical and administrative staffs at CERN and at other CMS institutes for their contributions to the success of the CMS effort. In addition, we gratefully acknowledge the computing centers and personnel of the Worldwide LHC Computing Grid and other centers for delivering so effectively the computing infrastructure essential to our analyses. Finally, we acknowledge the enduring support for the construction and operation of the LHC, the CMS detector, and the supporting computing infrastructure provided by the following funding agencies: SC (Armenia), BMBWF and FWF (Austria); FNRS and FWO (Belgium); CNPq, CAPES, FAPERJ, FAPERGS, and FAPESP (Brazil); MES and BNSF (Bulgaria); CERN; CAS, MoST, and NSFC (China); MINCIENCIAS (Colombia); MSES and CSF (Croatia); RIF (Cyprus); SENESCYT (Ecuador); ERC PRG and PSG, TARISTU24-TK10 and MoER TK202 (Estonia); Academy of Finland, MEC, and HIP (Finland); CEA and CNRS/IN2P3 (France); SRNSF (Georgia); BMFTR, DFG, and HGF (Germany); GSRI (Greece); MATE and NKFIH (Hungary); DAE and DST (India); IPM (Iran); SFI (Ireland); INFN (Italy); MSIT and NRF (Republic of Korea); MES (Latvia); LMTLT (Lithuania); MOE and UM (Malaysia); BUAP, CINVESTAV, CONACYT, LNS, SEP, and UASLP-FAI (Mexico); MOS (Montenegro); MBIE (New Zealand); PAEC (Pakistan); MSHE, NSC, and NAWA (Poland); FCT (Portugal); MESTD (Serbia); MICIU/AEI and PCTI (Spain); MOSTR (Sri Lanka); Swiss Funding Agencies (Switzerland); MST (Taipei); MHESI (Thailand); TUBITAK and TENMAK (Türkiye); NASU (Ukraine); STFC (United Kingdom); DOE and NSF (U.S.A.).

Individuals have received support from the Marie-Curie program and the European Research Council and Horizon 2020 Grant, contract Nos. 675440, 724704, 752730, 758316, 765710, 824093, 101115353, 101002207, 101001205, and COST Action CA16108 (European Union); the Leventis Foundation; the Alfred P. Sloan Foundation; the Alexander von Humboldt Foundation; the Science Committee, project no. 22rl-037 (Armenia); the Fonds pour la Formation à la Recherche dans l'Industrie et dans l'Agriculture (FRIA) and Fonds voor

JHEP10(2026)167

Wetenschappelijk Onderzoek contract No. 1228724N (Belgium); the Beijing Municipal Science & Technology Commission, No. Z191100007219010, the Fundamental Research Funds for the Central Universities, the Ministry of Science and Technology of China under Grant No. 2023YFA1605804, the Natural Science Foundation of China under Grant No. 12535004, and USTC Research Funds of the Double First-Class Initiative No. YD2030002017 (China); the Ministry of Education, Youth and Sports (MEYS) of the Czech Republic; the Shota Rustaveli National Science Foundation, grant FR-22-985 (Georgia); the Deutsche Forschungsgemeinschaft (DFG), among others, under Germany's Excellence Strategy — EXC 2121 "Quantum Universe" — 390833306, and under project number 400140256 — GRK2497; the Hellenic Foundation for Research and Innovation (HFRI), Project Number 2288 (Greece); the Hungarian Academy of Sciences, the New National Excellence Program — ÚNKP, the NKFIH research grants K 131991, K 138136, K 143460, K 143477, K 147557, K 146913, K 146914, K 147048, TKP2021-NKTA-64, and 2025-1.1.5-NEMZ_KI-2025-00004, and MATE KKP and KKPCs Research Excellence and Flagship Research Groups grants (Hungary); the Council of Science and Industrial Research, India; ICSC — National Research Center for High Performance Computing, Big Data and Quantum Computing, FAIR — Future Artificial Intelligence Research, and CUP I53D23001070006 (Mission 4 Component 1), funded by the NextGenerationEU program, the Italian Ministry of University and Research (MUR) under Bando PRIN 2022 — CUP I53C24002390006, PRIN PRIMULA 2022RBYK7T (Italy); the Latvian Council of Science; the Ministry of Science and Higher Education, project no. 2022/WK/14, and the National Science Center, contracts Opus 2021/41/B/ST2/01369, 2021/43/B/ST2/01552, 2023/49/B/ST2/03273, and the NAWA contract BPN/PPO/2021/1/00011 (Poland); the Fundação para a Ciência e a Tecnologia (Portugal); the National Priorities Research Program by Qatar National Research Fund; MICIU/AEI/10.13039/501100011033, ERDF/EU, "European Union NextGenerationEU/PRTR", projects PID2022-142604OB-C21, PID2022-139519OB-C21, PID2023-147706NB-I00, PID2023-148896NB-I00, PID2023-146983NB-I00, PID2023-147115NB-I00, PID2023-148418NB-C41, PID2023-148418NB-C42, PID2023-148418NB-C43, PID2023-148418NB-C44, PID2024-158190NB-C22, RYC2021-033305-I, RYC2024-048719-I, CNS2023-144781, CNS2024-154769 and Plan de Ciencia, Tecnología e Innovación de Asturias, Spain; the Chulalongkorn Academic into Its 2nd Century Project Advancement Project, the National Science, Research and Innovation Fund program IND_FF_68_369_2300_097, and the Program Management Unit for Human Resources & Institutional Development, Research and Innovation, grant B39G680009 (Thailand); the Eric & Wendy Schmidt Fund for Strategic Innovation through the CERN Next Generation Triggers project under grant agreement number SIF-2023-004; the Kavli Foundation; the Nvidia Corporation; the SuperMicro Corporation; the Welch Foundation, contract C-1845; and the Weston Havens Foundation (U.S.A.).

Data Availability Statement. Release and preservation of data used by the CMS Collaboration as the basis for publications is guided by the CMS data preservation, re-use and open access policy.

Code Availability Statement. The CMS core software is publicly available on GitHub.

JHEP10(2026)167

Open Access. This article is distributed under the terms of the Creative Commons Attribution License (CC-BY4.0), which permits any use, distribution and reproduction in any medium, provided the original author(s) and source are credited.

References

[1] CMS collaboration, *Observation of a new boson at a mass of 125 GeV with the CMS experiment at the LHC*, *Phys. Lett. B* **716** (2012) 30 [arXiv:1207.7235] [INSPIRE].

[2] CMS collaboration, *Observation of a new boson with mass near 125 GeV in pp collisions at $\sqrt{s} = 7$ and 8 TeV*, *JHEP* **06** (2013) 081 [arXiv:1303.4571] [INSPIRE].

[3] ATLAS collaboration, *Observation of a new particle in the search for the Standard Model Higgs boson with the ATLAS detector at the LHC*, *Phys. Lett. B* **716** (2012) 1 [arXiv:1207.7214] [INSPIRE].

[4] CMS collaboration, *Identification of heavy, energetic, hadronically decaying particles using machine-learning techniques*, 2020 *JINST* **15** P06005 [arXiv:2004.08262] [INSPIRE].

[5] CMS collaboration, *Performance of the mass-decorrelated* DeepDoubleX *classifier for double-b and double-c large-radius jets with the CMS detector*, CMS-DP-2022-041 (2022).

[6] ATLAS collaboration, *Identification of boosted Higgs bosons decaying into $b\bar{b}$ with neural networks and variable radius subjets in ATLAS*, ATL-PHYS-PUB-2020-019 (2020) [INSPIRE].

[7] ATLAS collaboration, *DeXTer: deep sets based neural networks for low-p_T $X \to b\bar{b}$ identification in ATLAS*, ATL-PHYS-PUB-2022-042 (2022) [INSPIRE].

[8] E.A. Moreno et al., *JEDI-net: a jet identification algorithm based on interaction networks*, *Eur. Phys. J. C* **80** (2020) 58 [arXiv:1908.05318] [INSPIRE].

[9] E.A. Moreno et al., *Interaction networks for the identification of boosted $H \to b\bar{b}$ decays*, *Phys. Rev. D* **102** (2020) 012010 [arXiv:1909.12285] [INSPIRE].

[10] H. Qu and L. Gouskos, *ParticleNet: jet tagging via particle clouds*, *Phys. Rev. D* **101** (2020) 056019 [arXiv:1902.08570] [INSPIRE].

[11] CMS collaboration, *Identification of highly Lorentz-boosted heavy particles using graph neural networks and new mass decorrelation techniques*, CMS-DP-2020-002 (2020).

[12] CMS collaboration, *Mass regression of highly-boosted jets using graph neural networks*, CMS-DP-2021-017 (2021) [INSPIRE].

[13] ATLAS collaboration, *Transformer neural networks for identifying boosted Higgs bosons decaying into $b\bar{b}$ and $c\bar{c}$ in ATLAS*, ATL-PHYS-PUB-2023-021 (2023) [INSPIRE].

[14] CMS collaboration, *Measurement of boosted Higgs bosons produced via vector boson fusion or gluon fusion in the $H \to b\bar{b}$ decay mode using LHC proton-proton collision data at $\sqrt{s} = 13$ TeV*, *JHEP* **12** (2024) 035 [arXiv:2407.08012] [INSPIRE].

[15] CMS collaboration, *Search for Higgs boson decay to a charm quark-antiquark pair in proton-proton collisions at $\sqrt{s} = 13$ TeV*, *Phys. Rev. Lett.* **131** (2023) 061801 [arXiv:2205.05550] [INSPIRE].

[16] CMS collaboration, *Search for nonresonant pair production of highly energetic Higgs bosons decaying to bottom quarks*, *Phys. Rev. Lett.* **131** (2023) 041803 [arXiv:2205.06667] [INSPIRE].

JHEP10(2026)167

[17] ATLAS collaboration, *Search for pair production of boosted Higgs bosons via vector-boson fusion in the $b\bar{b}b\bar{b}$ final state using pp collisions at $\sqrt{s} = 13$ TeV with the ATLAS detector*, *Phys. Lett. B* **858** (2024) 139007 [arXiv:2404.17193] [INSPIRE].

[18] CMS collaboration, *Search for a massive scalar resonance decaying to a light scalar and a Higgs boson in the four b quarks final state with boosted topology*, *Phys. Lett. B* **842** (2023) 137392 [arXiv:2204.12413] [INSPIRE].

[19] CMS collaboration, *Search for resonant pair production of Higgs bosons in the $b\bar{b}b\bar{b}$ final state using large-area jets in proton-proton collisions at $\sqrt{s} = 13$ TeV*, *JHEP* **02** (2025) 040 [arXiv:2407.13872] [INSPIRE].

[20] CMS collaboration, *Search for heavy resonances decaying to a pair of Lorentz-boosted Higgs bosons in final states with leptons and a bottom quark pair at $\sqrt{s} = 13$ TeV*, *JHEP* **05** (2022) 005 [arXiv:2112.03161] [INSPIRE].

[21] CMS collaboration, *Search for resonances decaying to three W bosons in the hadronic final state in proton-proton collisions at $\sqrt{s} = 13$ TeV*, *Phys. Rev. D* **106** (2022) 012002 [arXiv:2112.13090] [INSPIRE].

[22] CMS collaboration, *Search for resonances decaying to three W bosons in proton-proton collisions at $\sqrt{s} = 13$ TeV*, *Phys. Rev. Lett.* **129** (2022) 021802 [arXiv:2201.08476] [INSPIRE].

[23] ATLAS collaboration, *Anomaly detection search for new resonances decaying into a Higgs boson and a generic new particle X in hadronic final states using $\sqrt{s} = 13$ TeV pp collisions with the ATLAS detector*, *Phys. Rev. D* **108** (2023) 052009 [arXiv:2306.03637] [INSPIRE].

[24] L. de Oliveira et al., *Jet-images — deep learning edition*, *JHEP* **07** (2016) 069 [arXiv:1511.05190] [INSPIRE].

[25] P.T. Komiske, E.M. Metodiev and J. Thaler, *Energy flow networks: deep sets for particle jets*, *JHEP* **01** (2019) 121 [arXiv:1810.05165] [INSPIRE].

[26] F.A. Dreyer and H. Qu, *Jet tagging in the Lund plane with graph networks*, *JHEP* **03** (2021) 052 [arXiv:2012.08526] [INSPIRE].

[27] V. Mikuni and F. Canelli, *ABCNet: an attention-based method for particle tagging*, *Eur. Phys. J. Plus* **135** (2020) 463 [arXiv:2001.05311] [INSPIRE].

[28] A. Bogatskiy et al., *Lorentz group equivariant neural network for particle physics*, in *Proc. 37th International Conference on Machine Learning*, H. Daumé III and A. Singh eds., volume 119, (2020), p. 992 [arXiv:2006.04780] [INSPIRE].

[29] A. Bogatskiy et al., *Explainable equivariant neural networks for particle physics: PELICAN*, *JHEP* **03** (2024) 113 [arXiv:2307.16506] [INSPIRE].

[30] J. Brehmer et al., *A Lorentz-equivariant transformer for all of the LHC*, *SciPost Phys.* **19** (2025) 108 [arXiv:2411.00446] [INSPIRE].

[31] J. Spinner et al., *Lorentz-equivariant geometric algebra transformers for high-energy physics*, in the proceedings of the *38th conference on Neural Information Processing Systems*, Vancouver, Canada, 09–15 December 2024 [arXiv:2405.14806] [INSPIRE].

[32] H. Qu, C. Li and S. Qian, *Particle transformer for jet tagging*, in *Proc. 39th Int. Conf. on Machine Learning*, volume 162, (2022), p. 18281 [arXiv:2202.03772] [INSPIRE].

[33] A.J. Larkoski, I. Moult and B. Nachman, *Jet substructure at the Large Hadron Collider: a review of recent advances in theory and machine learning*, *Phys. Rept.* **841** (2020) 1 [arXiv:1709.04464] [INSPIRE].

JHEP10(2026)167

[34] A. Butter et al., *The machine learning landscape of top taggers*, *SciPost Phys.* **7** (2019) 014 [arXiv:1902.09914] [INSPIRE].

[35] L. Bradshaw, R.K. Mishra, A. Mitridate and B. Ostdiek, *Mass agnostic jet taggers*, *SciPost Phys.* **8** (2020) 011 [arXiv:1908.08959] [INSPIRE].

[36] J.A. Aguilar-Saavedra and B. Zaldívar, *Jet tagging made easy*, *Eur. Phys. J. C* **80** (2020) 530 [arXiv:2002.12320] [INSPIRE].

[37] J.A. Aguilar-Saavedra, F.R. Joaquim and J.F. Seabra, *Mass Unspecific Supervised Tagging (MUST) for boosted jets*, *JHEP* **03** (2021) 012 [*Erratum ibid.* **04** (2021) 133] [arXiv:2008.12792] [INSPIRE].

[38] J.A. Aguilar-Saavedra et al., *Gradient boosting MUST taggers for highly-boosted jets*, *Eur. Phys. J. Plus* **139** (2024) 1019 [arXiv:2305.04957] [INSPIRE].

[39] CMS collaboration, *Search for a massive resonance decaying into a Higgs boson and a W or Z boson in hadronic final states in proton-proton collisions at* $\sqrt{s} = 8$ *TeV*, *JHEP* **02** (2016) 145 [arXiv:1506.01443] [INSPIRE].

[40] G.C. Branco et al., *Theory and phenomenology of two-Higgs-doublet models*, *Phys. Rept.* **516** (2012) 1 [arXiv:1106.0034] [INSPIRE].

[41] N. Craig, J. Galloway and S. Thomas, *Searching for signs of the second Higgs doublet*, arXiv:1305.2424 [INSPIRE].

[42] F. Domingo and S. Paßehr, *About the bosonic decays of heavy Higgs states in the (N)MSSM*, *Eur. Phys. J. C* **82** (2022) 962 [arXiv:2207.05776] [INSPIRE].

[43] K.S. Agashe et al., *LHC signals from cascade decays of warped vector resonances*, *JHEP* **05** (2017) 078 [arXiv:1612.00047] [INSPIRE].

[44] K. Agashe et al., *Dedicated strategies for triboson signals from cascade decays of vector resonances*, *Phys. Rev. D* **99** (2019) 075016 [arXiv:1711.09920] [INSPIRE].

[45] H.-Y. Ren, L.-H. Xia and Y.-P. Kuang, *Model-independent probe of anomalous heavy neutral Higgs bosons at the LHC*, *Phys. Rev. D* **90** (2014) 115002 [arXiv:1404.6367] [INSPIRE].

[46] Y.-P. Kuang, H.-Y. Ren and L.-H. Xia, *Further investigation of the model-independent probe of heavy neutral Higgs bosons at LHC run 2*, *Chin. Phys. C* **40** (2016) 023101 [arXiv:1506.08007] [INSPIRE].

[47] J. Dolen et al., *Thinking outside the ROCs: Designing Decorrelated Taggers (DDT) for jet substructure*, *JHEP* **05** (2016) 156 [arXiv:1603.00027] [INSPIRE].

[48] F.A. Dreyer, G.P. Salam and G. Soyez, *The Lund jet plane*, *JHEP* **12** (2018) 064 [arXiv:1807.04758] [INSPIRE].

[49] CMS collaboration, *A method for correcting the substructure of multiprong jets using the Lund jet plane*, *JHEP* **11** (2025) 038 [arXiv:2507.07775] [INSPIRE].

[50] CMS collaboration, *Combination of searches for nonresonant Higgs boson pair production in proton-proton collisions at* $\sqrt{s} = 13$ *TeV*, *J. Phys. G* **53** (2026) 095001 [arXiv:2510.07527] [INSPIRE].

[51] CMS collaboration, *The CMS experiment at the CERN LHC*, 2008 *JINST* **3** S08004 [INSPIRE].

[52] CMS collaboration, *Development of the CMS detector for the CERN LHC run 3*, 2024 *JINST* **19** P05064 [arXiv:2309.05466] [INSPIRE].

JHEP10(2026)167

[53] CMS collaboration, *Performance of the CMS level-1 trigger in proton-proton collisions at $\sqrt{s} = 13$ TeV*, 2020 *JINST* **15** P10017 [arXiv:2006.10165] [INSPIRE].

[54] CMS collaboration, *The CMS trigger system*, 2017 *JINST* **12** P01020 [arXiv:1609.02366] [INSPIRE].

[55] CMS collaboration, *Performance of the CMS high-level trigger during LHC run 2*, 2024 *JINST* **19** P11021 [arXiv:2410.17038] [INSPIRE].

[56] CMS collaboration, *Electron and photon reconstruction and identification with the CMS experiment at the CERN LHC*, 2021 *JINST* **16** P05014 [arXiv:2012.06888] [INSPIRE].

[57] CMS collaboration, *Performance of the CMS muon detector and muon reconstruction with proton-proton collisions at $\sqrt{s} = 13$ TeV*, 2018 *JINST* **13** P06015 [arXiv:1804.04528] [INSPIRE].

[58] CMS collaboration, *Description and performance of track and primary-vertex reconstruction with the CMS tracker*, 2014 *JINST* **9** P10009 [arXiv:1405.6569] [INSPIRE].

[59] CMS Tracker Group collaboration, *The CMS phase-1 pixel detector upgrade*, 2021 *JINST* **16** P02027 [arXiv:2012.14304] [INSPIRE].

[60] CMS collaboration, *Track impact parameter resolution for the full pseudo rapidity coverage in the 2017 dataset with the CMS phase-1 pixel detector*, CMS-DP-2020-049 (2020).

[61] CMS collaboration, *2017 tracking performance plots*, CMS-DP-2017-015 (2017).

[62] CMS collaboration, *Particle-flow reconstruction and global event description with the CMS detector*, 2017 *JINST* **12** P10003 [arXiv:1706.04965] [INSPIRE].

[63] CMS collaboration, *Technical proposal for the Phase-II upgrade of the Compact Muon Solenoid*, CMS-TDR-15-02 (2015) [CERN-LHCC-2015-010] [DOI:10.17181/CERN.VU8I.D59J] [INSPIRE].

[64] CMS collaboration, *Offline secondary vertex reconstruction in the CMS detector*, *PoS* **LHCP2024** (2025) 236 [INSPIRE].

[65] M. Cacciari, G.P. Salam and G. Soyez, *The anti-k_t jet clustering algorithm*, *JHEP* **04** (2008) 063 [arXiv:0802.1189] [INSPIRE].

[66] M. Cacciari, G.P. Salam and G. Soyez, *FastJet user manual*, *Eur. Phys. J. C* **72** (2012) 1896 [arXiv:1111.6097] [INSPIRE].

[67] CMS collaboration, *Pileup removal algorithms*, CMS-PAS-JME-14-001 (2014) [INSPIRE].

[68] D. Bertolini, P. Harris, M. Low and N. Tran, *Pileup per particle identification*, *JHEP* **10** (2014) 059 [arXiv:1407.6013] [INSPIRE].

[69] CMS collaboration, *Pileup mitigation at CMS in 13 TeV data*, 2020 *JINST* **15** P09018 [arXiv:2003.00503] [INSPIRE].

[70] CMS collaboration, *Jet energy scale and resolution in the CMS experiment in pp collisions at 8 TeV*, 2017 *JINST* **12** P02014 [arXiv:1607.03663] [INSPIRE].

[71] S. Catani, Y.L. Dokshitzer, M.H. Seymour and B.R. Webber, *Longitudinally invariant K_t clustering algorithms for hadron hadron collisions*, *Nucl. Phys. B* **406** (1993) 187 [INSPIRE].

[72] S.D. Ellis and D.E. Soper, *Successive combination jet algorithm for hadron collisions*, *Phys. Rev. D* **48** (1993) 3160 [hep-ph/9305266] [INSPIRE].

[73] Y.L. Dokshitzer, G.D. Leder, S. Moretti and B.R. Webber, *Better jet clustering algorithms*, *JHEP* **08** (1997) 001 [hep-ph/9707323] [INSPIRE].

JHEP10(2026)167

[74] M. Wobisch and T. Wengler, *Hadronization corrections to jet cross-sections in deep inelastic scattering*, in the proceedings of the *Workshop on Monte Carlo Generators for HERA Physics (Plenary Starting Meeting)*, Hamburg, Germany, 27–30 April 1998 [hep-ph/9907280] [INSPIRE].

[75] A.J. Larkoski, S. Marzani, G. Soyez and J. Thaler, *Soft drop*, *JHEP* **05** (2014) 146 [arXiv:1402.2657] [INSPIRE].

[76] E. Bols et al., *Jet flavour classification using DeepJet*, 2020 *JINST* **15** P12012 [arXiv:2008.10519] [INSPIRE].

[77] CMS collaboration, *Performance of missing transverse momentum reconstruction in proton-proton collisions at* $\sqrt{s} = 13$ *TeV using the CMS detector*, 2019 *JINST* **14** P07004 [arXiv:1903.06078] [INSPIRE].

[78] G. Louppe, M. Kagan and K. Cranmer, *Learning to pivot with adversarial networks*, in *Advances in neural information processing systems*, I. Guyon et al. eds., volume 30, Curran Associates Inc. (2017) [arXiv:1611.01046] [INSPIRE].

[79] C. Shimmin et al., *Decorrelated jet substructure tagging using adversarial neural networks*, *Phys. Rev. D* **96** (2017) 074034 [arXiv:1703.03507] [INSPIRE].

[80] CMS collaboration, *A deep neural network to search for new long-lived particles decaying to jets*, *Mach. Learn. Sci. Tech.* **1** (2020) 035012 [arXiv:1912.12238] [INSPIRE].

[81] G. Kasieczka and D. Shih, *Robust jet classifiers through distance correlation*, *Phys. Rev. Lett.* **125** (2020) 122001 [arXiv:2001.05310] [INSPIRE].

[82] J. Alwall et al., *The automated computation of tree-level and next-to-leading order differential cross sections, and their matching to parton shower simulations*, *JHEP* **07** (2014) 079 [arXiv:1405.0301] [INSPIRE].

[83] S. Bolognesi et al., *On the spin and parity of a single-produced resonance at the LHC*, *Phys. Rev. D* **86** (2012) 095031 [arXiv:1208.4018] [INSPIRE].

[84] Particle Data Group collaboration, *Review of particle physics*, *Phys. Rev. D* **110** (2024) 030001 [INSPIRE].

[85] T. Sjöstrand et al., *An introduction to PYTHIA 8.2*, *Comput. Phys. Commun.* **191** (2015) 159 [arXiv:1410.3012] [INSPIRE].

[86] M. Cacciari and G.P. Salam, *Pileup subtraction using jet areas*, *Phys. Lett. B* **659** (2008) 119 [arXiv:0707.1378] [INSPIRE].

[87] P. Nason, *A new method for combining NLO QCD with shower Monte Carlo algorithms*, *JHEP* **11** (2004) 040 [hep-ph/0409146] [INSPIRE].

[88] S. Frixione, P. Nason and C. Oleari, *Matching NLO QCD computations with parton shower simulations: the POWHEG method*, *JHEP* **11** (2007) 070 [arXiv:0709.2092] [INSPIRE].

[89] S. Alioli, P. Nason, C. Oleari and E. Re, *A general framework for implementing NLO calculations in shower Monte Carlo programs: the POWHEG BOX*, *JHEP* **06** (2010) 043 [arXiv:1002.2581] [INSPIRE].

[90] E. Bagnaschi, G. Degrassi, P. Slavich and A. Vicini, *Higgs production via gluon fusion in the POWHEG approach in the SM and in the MSSM*, *JHEP* **02** (2012) 088 [arXiv:1111.2854] [INSPIRE].

[91] F.A. Dreyer and A. Karlberg, *Vector-boson fusion Higgs pair production at* N^3LO, *Phys. Rev. D* **98** (2018) 114016 [arXiv:1811.07906] [INSPIRE].

JHEP10(2026)167

[92] M. Grazzini et al., *Higgs boson pair production at NNLO with top quark mass effects*, *JHEP* **05** (2018) 059 [arXiv:1803.02463] [INSPIRE].

[93] S. Dawson, S. Dittmaier and M. Spira, *Neutral Higgs boson pair production at hadron colliders: QCD corrections*, *Phys. Rev. D* **58** (1998) 115012 [hep-ph/9805244] [INSPIRE].

[94] D. de Florian and J. Mazzitelli, *Higgs boson pair production at next-to-next-to-leading order in QCD*, *Phys. Rev. Lett.* **111** (2013) 201801 [arXiv:1309.6594] [INSPIRE].

[95] D. de Florian and J. Mazzitelli, *Higgs pair production at next-to-next-to-leading logarithmic accuracy at the LHC*, *JHEP* **09** (2015) 053 [arXiv:1505.07122] [INSPIRE].

[96] J. Baglio et al., *Gluon fusion into Higgs pairs at NLO QCD and the top mass scheme*, *Eur. Phys. J. C* **79** (2019) 459 [arXiv:1811.05692] [INSPIRE].

[97] S. Borowka et al., *Higgs boson pair production in gluon fusion at next-to-leading order with full top-quark mass dependence*, *Phys. Rev. Lett.* **117** (2016) 012001 [*Erratum ibid.* **117** (2016) 079901] [arXiv:1604.06447] [INSPIRE].

[98] D.Y. Shao, C.S. Li, H.T. Li and J. Wang, *Threshold resummation effects in Higgs boson pair production at the LHC*, *JHEP* **07** (2013) 169 [arXiv:1301.1245] [INSPIRE].

[99] CMS collaboration, *Extraction and validation of a new set of CMS PYTHIA8 tunes from underlying-event measurements*, *Eur. Phys. J. C* **80** (2020) 4 [arXiv:1903.12179] [INSPIRE].

[100] NNPDF collaboration, *Parton distributions for the LHC run II*, *JHEP* **04** (2015) 040 [arXiv:1410.8849] [INSPIRE].

[101] NNPDF collaboration, *Parton distributions from high-precision collider data*, *Eur. Phys. J. C* **77** (2017) 663 [arXiv:1706.00428] [INSPIRE].

[102] GEANT4 collaboration, *GEANT4 — a simulation toolkit*, *Nucl. Instrum. Meth. A* **506** (2003) 250 [INSPIRE].

[103] A. Vaswani et al., *Attention is all you need*, in the proceedings of the *31st International Conference on Neural Information Processing Systems*, Long Beach, U.S.A., 04–09 December 2017 [arXiv:1706.03762] [INSPIRE].

[104] H. Touvron et al., *Going deeper with image transformers*, in the proceedings of the *2021 IEEE/CVF International Conference on Computer Vision (ICCV)*, (2021) [DOI:10.1109/iccv48922.2021.00010] [arXiv:2103.17239].

[105] J. Bridle, *Training stochastic model recognition algorithms as networks can lead to maximum mutual information estimation of parameters*, in *Advances in Neural Information Processing Systems*, D. Touretzky ed., volume 2, Morgan-Kaufmann (1989), p. 211.

[106] CMS collaboration, *Identification of heavy-flavour jets with the CMS detector in pp collisions at 13 TeV*, 2018 *JINST* **13** P05011 [arXiv:1712.07158] [INSPIRE].

[107] H. Qu, *Weaver: a machine learning R&D framework for high energy physics applications*, https://github.com/hqucms/weaver-core, accessed on 4 June 2025.

[108] A. Paszke et al., *PyTorch: an imperative style, high-performance deep learning library*, in *Advances in Neural Information Processing Systems*, volume 32, Curran Associates Inc. (2019), p. 8024 [arXiv:1912.01703] [INSPIRE].

[109] M.R. Zhang, J. Lucas, G. Hinton and J. Ba, *Lookahead optimizer: k steps forward, 1 step back*, in *Advances in neural information processing systems*, H. Wallach et al. eds., volume 32, Curran Associates Inc. (2019) [arXiv:1907.08610].

JHEP10(2026)167

[110] L. Liu et al., *On the variance of the adaptive learning rate and beyond*, in *Proc. Int. Conf. on Learning Representations (ICLR)* (2020) [arXiv:1908.03265].

[111] CMS collaboration, *Calibration of the jet mass scale using boosted W bosons and top quarks*, CMS-DP-2023-044 (2023).

[112] CMS collaboration, *Calibration of the jet mass scale using boosted W bosons and top quarks for data taken in 2022*, CMS-DP-2025-052 (2025).

[113] K. He, X. Zhang, S. Ren and J. Sun, *Deep residual learning for image recognition*, in *Proc. IEEE Conf. on Computer Vision and Pattern Recognition (CVPR)*, (2016), p. 770 [DOI:10.1109/CVPR.2016.90] [arXiv:1512.03385] [INSPIRE].

[114] CMS collaboration, *Search for heavy scalar resonances decaying to Lorentz-boosted Higgs and Higgs-like bosons in the* $\mathrm{b\bar{b}4q}$ *final state at* $\sqrt{s} = 13$ *TeV*, *JHEP* **08** (2026) 050 [arXiv:2602.00273] [INSPIRE].

[115] J. Lin, *Divergence measures based on the Shannon entropy*, *IEEE Trans. Info. Theor.* **37** (1991) 145 [INSPIRE].

[116] S. Kullback and R.A. Leibler, *On information and sufficiency*, *Annals Math. Statist.* **22** (1951) 79 [INSPIRE].

[117] CMS collaboration, *Performance of heavy-flavour jet identification in Lorentz-boosted topologies in proton-proton collisions at* $\sqrt{s} = 13$ *TeV*, 2025 *JINST* **20** P11006 [arXiv:2510.10228] [INSPIRE].

[118] *CMS data preservation, re-use and open access policy*, DOI:10.7483/OPENDATA.CMS.1BNU.8V1W.

[119] *CMS core software GitHub repository*, https://github.com/cms-sw/cmssw.

JHEP10(2026)167

The CMS collaboration

A. Hayrapetyan[1], V. Makarenko[1], A. Tumasyan[1,a], W. Adam[2], L. Benato[2], T. Bergauer[2], M. Dragicevic[2], C. Giordano[2], P.S. Hussain[2], M. Jeitler[2,b], N. Krammer[2], A. Li[2], D. Liko[2], M. Matthewman[2], J. Schieck[2,b], R. Schöfbeck[2,b], M. Shooshtari[2], M. Sonawane[2], W. Waltenberger[2], C.E. Wulz[2,b], T. Janssen[3], H. Kwon[3], D. Ocampo Henao[3], T. Van Laer[3], P. Van Mechelen[3], J. Bierkens[4], N. Breugelmans[4], J. D'Hondt[4], S. Dansana[4], A. De Moor[4], M. Delcourt[4], F. Heyen[4], Y. Hong[4], P. Kashko[4], S. Lowette[4], I. Makarenko[4], D. Müller[4], J. Song[4], S. Tavernier[4], M. Tytgat[4,c], G.P. Van Onsem[4], S. Van Putte[4], D. Vannerom[4], B. Bilin[5], B. Clerbaux[5], A.K. Das[5], I. De Bruyn[5], G. De Lentdecker[5], H. Evard[5], L. Favart[5], P. Gianneios[5], A. Khalilzadeh[5], F.A. Khan[5], A. Malara[5], M.A. Shahzad[5], A. Sharma[5], L. Thomas[5], M. Vanden Bemden[5], C. Vander Velde[5], P. Vanlaer[5], F. Zhang[5], M. De Coen[6], D. Dobur[6], G. Gokbulut[6], D. Marckx[6], K. Skovpen[6], A.M. Tomaru[6], N. Van Den Bossche[6], J. van der Linden[6], J. Vandenbroeck[6], L. Wezenbeek[6], H. Aarup Petersen[7], S. Bein[7], A. Benecke[7], A. Bethani[7], G. Bruno[7], A. Cappati[7], J. De Favereau De Jeneret[7], C. Delaere[7], F. Gameiro Casalinho[7], A. Giammanco[7], A.O. Guzel[7], V. Lemaitre[7], J. Lidrych[7], P. Malek[7], P. Mastrapasqua[7], S. Turkcapar[7], G. Alves[8], M. Barroso Ferreira Filho[8], E. Coelho[8], C. Hensel[8], D. Matos Figueiredo[8], T. Menezes De Oliveira[8], C. Mora Herrera[8], P. Rebello Teles[8], M. Soeiro[8], E.J. Tonelli Manganote[8,d], A. Vilela Pereira[8], W.L. Aldá Júnior[9], H. Brandao Malbouisson[9], W. Carvalho[9], J. Chinellato[9,e], M. Costa Reis[9], E.M. Da Costa[9], G.G. Da Silveira[9,f], D. De Jesus Damiao[9], S. Fonseca De Souza[9], R. Gomes De Souza[9], S. Jesus[9], T. Laux Kuhn[9,f], M. Macedo[9], K. Mota Amarilo[9], L. Mundim[9], H. Nogima[9], J.P. Pinheiro[9], A. Santoro[9], A. Sznajder[9], M. Thiel[9], F. Torres Da Silva De Araujo[9,g], C.A. Bernardes[10,f], L. Calligaris[10], F. Damas[10], E. De Moraes Gregores[10], B. Lopes Da Costa[10], I. Maietto Silverio[10], P.G. Mercadante[10], S.F. Novaes[10], B. Orzari[10], S. Padula[10], V. Scheurer[10], T. Tomei[10], A. Aleksandrov[11], G. Antchev[11], P. Danev[11], R. Hadjiiska[11], P. Iaydjiev[11], M. Shopova[11], G. Sultanov[11], A. Dimitrov[12], L. Litov[12], B. Pavlov[12], P. Petkov[12], A. Petrov[12], D. Abbaneo[13], C. Amendola[13], R. Ardino[13], E. Auffray[13], J. Baechler[13], D. Barney[13], J. Bendavid[13], M. Bianco[13], A. Bocci[13], L. Borgonovi[13], C. Botta[13], A. Bragagnolo[13], C.E. Brown[13], C. Caillol[13], G. Cerminara[13], P. Connor[13], K. Cormier[13], D. D'Enterria[13], A. Dabrowski[13], A. David Tinoco Mendes[13], A. De Roeck[13], M.M. Defranchis[13], M. Deile[13], M. Dobson[13], P.J. Fernández Manteca[13], B.A. Fontana Santos Alves[13], E. Fontanesi[13], W. Funk[13], A. Gaddi[13], S. Giani[13], D. Gigi[13], K. Gill[13], F. Glege[13], M. Glowacki[13], A. Gruber[13], J. Hegeman[13], J.K. Heikkilä[13], R. Hofsaess[13], B. Huber[13], T. James[13], P. Janot[13], O. Kaluzinska[13], O. Karacheban[13,h], G. Karathanasis[13], S. Laurila[13], P. Lecoq[13], E. Leutgeb[13], C. Lourenco[13], A.m. Lyon[13], M. Magherini[13], L. Malgeri[13], M. Mannelli[13], A. Mehta[13], F. Meijers[13], J.A. Merlin[13], S. Mersi[13], E. Meschi[13], M. Migliorini[13], F. Monti[13], F. Moortgat[13], M. Mulders[13], M. Musich[13], I. Neutelings[13], S. Orfanelli[13], F. Pantaleo[13], M. Pari[13], G. Petrucciani[13], A. Pfeiffer[13], M. Pierini[13], M. Pitt[13], H. Qu[13], D. Rabady[13], A. Reimers[13], B. Ribeiro Lopes[13], F. Riti[13], P. Rosado[13], M. Rovere[13], H. Sakulin[13], R. Salvatico[13], S. Sanchez Cruz[13], S. Scarfi[13], M. Selvaggi[13], K. Shchelina[13], P. Silva[13], P. Sphicas[13,i],

JHEP10(2026)167

A.G. Stahl Leiton[13], A. Steen[13], S. Summers[13], D. Treille[13], P. Tropea[13], E. Vernazza[13], J. Wanczyk[13,j], S. Wuchterl[13], M. Zarucki[13], P. Zehetner[13], P. Zejdl[13], G. Zevi Della Porta[13], S. Keshri[14], D.N. Laroze Navarrete[14], S. Thakur[14], W. Brooks[15], T. Cheng[16], T. Javaid[16], L. Wang[16], L. Yuan[16], Z. Hu[17], Z. Liang[17], J. Liu[17], X. Wang[17], H. Yang[17], G.M. Chen[18,k], H.S. Chen[18,k], M. Chen[18,k], Y. Chen[18], Q. Hou[18], X. Hou[18], F. Iemmi[18], C.H. Jiang[18], H. Liao[18], G. Liu[18], Z. Liu[18,l], J.n. Song[18,l], S. Song[18], J. Tao[18], C. Wang[18,k], J. Wang[18], H. Zhang[18], J. Zhao[18], A. Agapitos[19], Y. Ban[19], A. Carvalho Antunes De Oliveira[19], S. Deng[19], D. Fu[19], B. Guo[19], Q. Guo[19], C. Jiang[19], A. Levin[19], C. Li[19], Q. Li[19], Y. Mao[19], S. Qian[19], S.J. Qian[19], X. Qin[19], C. Quaranta[19], X. Sun[19], D. Wang[19], J. Wang[19], M. Zhang[19], Y. Zhao[19], C. Zhou[19], S. Yang[20], Z. You[21], K. Jaffel[22], N. Lu[22], G. Bauer[23,m,n], Z. Cui[23,n], B. Li[23,o], H. Wang[23], K. Yi[23,p], J. Zhang[23], Y. Li[24], Y. Zhou[24,q], Z. Lin[25], C. Lu[25], M. Xiao[25,r], C. Avila[26], D.A. Barbosa Trujillo[26], A. Cabrera[26], C. Florez[26], J. Fraga[26], J.A. Reyes Vega[26], C. Rendón[27], M. Rodriguez[27], A.A. Ruales Barbosa[27], J.D. Ruiz Alvarez[27], N. Godinovic[28], D. Lelas[28], A. Sculac[28], M. Kovac[29], A. Petkovic[29], T. Sculac[29], P. Bargassa[30], V. Brigljevic[30], B.K. Chitroda[30], D. Ferencek[30], K. Jakovcic[30], A. Starodumov[30], T. Susa[30], A. Attikis[31], K. Christoforou[31], S. Konstantinou[31], C. Leonidou[31], L. Paizanos[31], F. Ptochos[31], P.A. Razis[31], H. Rykaczewski[31], H. Saka[31], A. Stepennov[31], M. Finger[32], M. Finger Jr.[32], E. Ayala[33], E. Carrera Jarrin[34], S. Elgammal[35,s], A. Ellithi Kamel[35,t], A. Hussein[36], H. Mohammed[36], M. Kadastik[37], T. Lange[37], C. Nielsen[37], J. Pata[37], M. Raidal[37], N. Seeba[37], L. Tani[37], E. Brücken[38], A. Milieva[38], K. Osterberg[38], M. Voutilainen[38], F.I. Garcia Fuentes[39], P. Inkaew[39], K.T.S. Kallonen[39], R. Kumar Verma[39], T. Lampén[39], K. Lassila-Perini[39], B. Lehtela[39], S. Lehti[39], T. Lindén[39], N.R. Mancilla Xinto[39], M. Myllymäki[39], M.m. Rantanen[39], S. Saariokari[39], N.T. Toikka[39], J. Tuominiemi[39], N. Bin Norjoharuddeen[40], H. Kirschenmann[40], P.R. Luukka[40], H. Petrow[40], M. Besancon[41], F. Couderc[41], M. Dejardin[41], D. Denegri[41], P. Devouge[41], J.L. Faure[41], F. Ferri[41], P. Gaigne[41], S. Ganjour[41], P. Gras[41], G. Hamel de Monchenault[41], M. Kumar[41], V. Lohezic[41], Y. Maidannyk[41], J. Malcles[41], F. Orlandi[41], L. Portales[41], S. Ronchi[41], M.Ö. Sahin[41], A. Savoy-Navarro[41,u], P. Simkina[41], M. Titov[41], M. Tornago[41], R. Amella Ranz[42], F. Beaudette[42], G. Boldrini[42], P. Busson[42], C. Charlot[42], M. Chiusi[42], T.D. Cuisset[42], O. Davignon[42], A. De Wit[42], T. Debnath[42], I.T. Ehle[42], S. Ghosh[42], A. Gilbert[42], R. Granier de Cassagnac[42], L. Kalipoliti[42], M. Manoni[42], M. Nguyen[42], S. Obraztsov[42], C. Ochando[42], R. Salerno[42], J.B. Sauvan[42], Y. Sirois[42], G. Sokmen[42], L. Urda Gómez[42], A. Zabi[42], A. Zghiche[42], J.L. Agram[43,v], J. Andrea[43], D. Bloch[43], J.M. Brom[43], E.C. Chabert[43], C. Collard[43], G. Coulon[43], S. Falke[43], U. Goerlach[43], R. Haeberle[43], A.C. Le Bihan[43], M. Meena[43], O. Poncet[43], G. Saha[43], P. Vaucelle[43], A. Di Florio[44], D. Amram[45], S. Beauceron[45], B. Blancon[45], G. Boudoul[45], N. Chanon[45], D. Contardo[45], P. Depasse[45], H. El Mamouni[45], J. Fay[45], S. Gascon[45], M. Gouzevitch[45], C. Greenberg[45], G. Grenier[45], B. Ille[45], E. Jourd'Huy[45], M. Lethuillier[45], B. Massoteau[45], L. Mirabito[45], A. Purohit[45], M. Vander Donckt[45], J. Xiao[45], I. Bagaturia[46,w], I. Lomidze[46], Z. Tsamalaidze[46,x], V. Botta[47], S. Consuegra Rodríguez[47], L. Feld[47], K. Klein[47], M. Lipinski[47], P. Nattland[47], V. Oppenländer[47], A. Pauls[47], D. Pérez Adán[47],

JHEP10(2026)167

N. Röwert[47], C. Daumann[48], S. Diekmann[48], N. Eich[48], D. Eliseev[48], F. Engelke[48], J. Erdmann[48], M. Erdmann[48], B. Fischer[48], T. Hebbeker[48], K. Hoepfner[48], F. Ivone[48], A. Jung[48], N. Kumar[48], M.y. Lee[48], F. Mausolf[48], M. Merschmeyer[48], A. Meyer[48], A. Pozdnyakov[48], W. Redjeb[48], H. Reithler[48], U. Sarkar[48], V. Sarkisovi[48], A. Schmidt[48], C. Seth[48], A. Sharma[48], J.L. Spah[48], V. Vaulin[48], S. Zaleski[48], M.R. Beckers[49], C. Dziwok[49], G. Flügge[49], N. Hoeflich[49], T. Kress[49], A. Nowack[49], O. Pooth[49], A. Stahl[49], A. Zotz[49], A. Abel[50], M. Aldaya Martin[50], J. Alimena[50], S. Amoroso[50], Y. An[50], I. Andreev[50], J. Bach[50], S. Baxter[50], M. Bayatmakou[50], H. Becerril Gonzalez[50], O. Behnke[50], A. Belvedere[50], F. Blekman[50,y], K. Borras[50,z], A. Campbell[50], S. Chatterjee[50], L.X. Coll Saravia[50], G. Eckerlin[50], D. Eckstein[50], E. Gallo[50,y], A. Geiser[50], M. Guthoff[50], A. Hinzmann[50], L. Jeppe[50], M. Kasemann[50], C. Kleinwort[50], R. Kogler[50], M. Komm[50], D. Krücker[50], W. Lange[50], D. Leyva Pernia[50], K.y. Lin[50], K. Lipka[50,aa], W. Lohmann[50,h], J. Malvaso[50], R. Mankel[50], I.A. Melzer-Pellmann[50], M. Mendizabal Morentin[50], A.B. Meyer[50], G. Milella[50], K. Moral Figueroa[50], A. Mussgiller[50], L.P. Nair[50], J. Niedziela[50], A. Nürnberg[50], J. Park[50], E. Ranken[50], A. Raspereza[50], D. Rastorguev[50], L. Rygaard[50], M. Scham[50,ab,z], S. Schnake[50,z], P. Schütze[50], C. Schwanenberger[50,y], D. Schwarz[50], D. Selivanova[50], K. Sharko[50], M. Shchedrolosiev[50], D. Stafford[50], M. Torkian[50], A. Ventura Barroso[50], R. Walsh[50], D. Wang[50], Q. Wang[50], K. Wichmann[50], L. Wiens[50,z], C. Wissing[50], Y. Yang[50], S. Zakharov[50], A. Zimermmane Castro Santos[50], A.R. Alves Andrade[51], M. Antonello[51], S. Bollweg[51], M. Bonanomi[51], L. Ebeling[51], K. El Morabit[51], Y. Fischer[51], M. Frahm[51], E. Garutti[51], A. Grohsjean[51], A.A. Guvenli[51], J. Haller[51], D. Hundhausen[51], G. Kasieczka[51], P. Keicher[51], R. Klanner[51], W. Korcari[51], T. Kramer[51], C.c. Kuo[51], F. Labe[51], J. Lange[51], A. Lobanov[51], J. Matthiesen[51], L. Moureaux[51], K. Nikolopoulos[51], A. Paasch[51], K.J. Pena Rodriguez[51], N. Prouvost[51], B. Raciti[51], M. Rieger[51], D. Savoiu[51], P. Schleper[51], M. Schröder[51], J. Schwandt[51], M. Sommerhalder[51], H. Stadie[51], G. Steinbrück[51], R. Ward[51], B. Wiederspan[51], M. Wolf[51], C. Yede[51], J. Ahäuser[52], S. Brommer[52], A. Brusamolino[52], E. Butz[52], Y.M. Chen[52], T. Chwalek[52], A. Dierlamm[52], G.G. Dincer[52], D. Druzhkin[52], U. Elicabuk[52], N. Faltermann[52], M. Giffels[52], A. Gottmann[52], F. Hartmann[52,ac], M. Horzela[52], F. Hummer[52], U. Husemann[52], J. Kieseler[52], M. Klute[52], R. Kunnilan Muhammed Rafeek[52], O. Lavoryk[52], J.M. Lawhorn[52], A. Lintuluoto[52], S. Maier[52], A.A. Monsch[52], M. Mormile[52], T. Müller[52], E. Pfeffer[52], M. Presilla[52], G. Quast[52], K. Rabbertz[52], B. Regnery[52], R. Schmieder[52], N. Shadskiy[52], I. Shvetsov[52], H.J. Simonis[52], L. Sowa[52], L. Stockmeier[52], K. Tauqeer[52], M. Toms[52], B. Topko[52], N. Trevisani[52], C. Verstege[52], T. Voigtländer[52], R.F. Von Cube[52], J. Von Den Driesch[52], M. Wassmer[52], C. Winter[52], R. Wolf[52], W.D. Zeuner[52], X. Zuo[52], G. Anagnostou[53], G. Daskalakis[53], A. Kyriakis[53], G. Melachroinos[54], Z. Painesis[54], I. Paraskevas[54], N. Saoulidou[54], K. Theofilatos[54], E. Tziaferi[54], E. Tzovara[54], K. Vellidis[54], I. Zisopoulos[54], T. Chatzistavrou[55], G. Karapostoli[55], K. Kousouris[55], E. Siamarkou[55], G. Tsipolitis[55], I. Bestintzanos[56], I. Evangelou[56], C. Foudas[56], P. Katsoulis[56], P. Kokkas[56], P.G. Kosmoglou Kioseoglou[56], N. Manthos[56], I. Papadopoulos[56], J. Strologas[56], C. Hajdu[57], D. Horvath[57,ad,ae], K. Márton[57], A.J. Rádl[57,af], F. Sikler[57], V. Veszpremi[57], M. Csanad[58], K. Farkas[58],

JHEP10(2026)167

A. Fehérkuti[58,ag], M.M.A. Gadallah[58,ah], Á. Kadlecsik[58], M. León Coello[58], G. Pasztor[58], G.I. Veres[58], B. Ujvari[59], G. Zilizi[59], G. Bencze[60], S. Czellar[60], J. Molnar[60], Z. Szillasi[60], T.F. Csorgo[61,ag], F. Nemes[61,ag], T. Novak[61], I. Szanyi[61,ai], S. Bahinipati[62], S. Nayak[62], R. Raturi[62], S. Bansal[63], S.B. Beri[63], V. Bhatnagar[63], S. Chauhan[63], N. Dhingra[63,aj], A. Kaur[63], H. Kaur[63], M. Kaur[63], S. Kumar[63], T. Sheokand[63], J. Singh[63], A. Singla[63], A. Bhardwaj[64], A. Chhetri[64], B.C. Choudhary[64], A. Kumar[64], A. Kumar[64], M. Naimuddin[64], S. Phor[64], K. Ranjan[64], M.K. Saini[64], P. Palni[65], S. Acharya[66,ak], B. Gomber[66], S. Mukherjee[67], S. Bhattacharya[68], S. Das Gupta[68], S. Dutta[68], S. Dutta[68], S. Sarkar[68], M.M. Ameen[69], P.K. Behera[69], S. Chatterjee[69], G. Dash[69], A. Dattamunsi[69], P. Jana[69], P. Kalbhor[69], S. Kamble[69], J.R. Komaragiri[69,al], T. Mishra[69], P.R. Pujahari[69], A.K. Sikdar[69], R.K. Singh[69], P. Verma[69], S. Verma[69], A. Vijay[69], B.K. Sirasva[70], L. Bhatt[71], S. Dugad[71], G.B. Mohanty[71], M. Shelake[71], P. Suryadevara[71], A. Bala[72], S. Banerjee[72], S. Barman[72,am], R.M. Chatterjee[72], M. Guchait[72], S. Jain[72], A. Jaiswal[72], S. Kumar[72], M. Maity[72,am], G. Majumder[72], K. Mazumdar[72], S. Parolia[72], R. Saxena[72], A. Thachayath[72], D. Maity[73,an], P. Mal[73], K. Naskar[73,an], A. Nayak[73,an], K. Pal[73], P. Sadangi[73], S.K. Swain[73], S. Varghese[73,an], D. Vats[73,an], S. Dube[74], P. Hazarika[74], B. Kansal[74], A. Laha[74], R. Sharma[74], S. Sharma[74], K.Y. Vaish[74], S. Ghosh[75], H. Bakhshiansohi[76,ao], A. Jafari[76,ap], V. Sedighzadeh Dalavi[76], M. Zeinali[76,aq], S. Bashiri[77], S. Chenarani[77,ar], S.M. Etesami[77], Y. Hosseini[77], M. Khakzad[77], E. Khazaie[77], M. Mohammadi Najafabadi[77], S. Tizchang[77,as], M. Felcini[78], M. Grunewald[78], M. Abbrescia[79a,79b], M. Barbieri[79a,79b], M. Buonsante[79a,79b], A. Colaleo[79a,79b], D. Creanza[79a,79c], N. De Filippis[79a,79c], M. De Palma[79a,79b], W. Elmetenawee[79a,79b,at], N. Ferrara[79a,79c], L. Fiore[79a], L. Generoso[79a,79b], L. Longo[79a], M. Louka[79a,79b], G. Maggi[79a,79c], M. Maggi[79a], I. Margjeka[79a], V. Mastrapasqua[79a,79b], S. My[79a,79b], F. Nenna[79a,79b], S. Nuzzo[79a,79b], A. Pellecchia[79a,79b], A. Pompili[79a,79b], G. Pugliese[79a,79c], R. Radogna[79a,79b], D. Ramos[79a], A. Ranieri[79a], L. Silvestris[79a], F.M. Simone[79a,79c], Ü. Sözbilir[79a], A. Stamerra[79a,79b], D. Troiano[79a,79b], R. Venditti[79a,79b], P. Verwilligen[79a], A. Zaza[79a,79b], C. Battilana[80a,80b], D. Bonacorsi[80a,80b], P. Capiluppi[80a,80b], F.R. Cavallo[80a], M. Cuffiani[80a,80b], G.M. Dallavalle[80a], T. Diotalevi[80a,80b], F. Fabbri[80a], R. Farinelli[80a], D. Fasanella[80a], P. Giacomelli[80a], L. Giommi[80a,80b], C. Grandi[80a], L. Guiducci[80a,80b], S. Lo Meo[80a,au], M. Lorusso[80a,80b], L. Lunerti[80a], S. Marcellini[80a], G. Masetti[80a], F. Navarria[80a,80b], G. Paggi[80a,80b], A. Perrotta[80a], A. Rossi[80a,80b], S. Rossi Tisbeni[80a,80b], G.P. Siroli[80a,80b], S. Costa[81a,81b,av], A. Di Mattia[81a], A. Lapertosa[81a], R. Potenza[81a,81b], A. Tricomi[81a,81b,av], J. Altork[82a,82b], P. Assiouras[82a], G. Barbagli[82a], G. Bardelli[82a], M. Bartolini[82a,82b], A. Calandri[82a,82b], B. Camaiani[82a,82b], A. Cassese[82a], R. Ceccarelli[82a], V. Ciulli[82a,82b], C. Civinini[82a], R. D'Alessandro[82a,82b], L. Damenti[82a,82b], E. Focardi[82a,82b], T. Kello[82a], G. Latino[82a,82b], P. Lenzi[82a,82b], M. Lizzo[82a], M. Meschini[82a], S. Paoletti[82a], A. Papanastassiou[82a,82b], G. Sguazzoni[82a], L. Viliani[82a], L. Benussi[83], S. Colafranceschi[83,aw], S. Meola[83,ax], D. Piccolo[83], M. Alves Gallo Pereira[84a], F. Ferro[84a], E. Robutti[84a], S. Tosi[84a,84b], A. Benaglia[85a], F. Brivio[85a], V. Camagni[85a,85b], F. Cetorelli[85a,85b], F. De Guio[85a,85b], M.E. Dinardo[85a,85b], P. Dini[85a], S. Gennai[85a], R. Gerosa[85a,85b], A. Ghezzi[85a,85b], P. Govoni[85a,85b], L. Guzzi[85a], M.R. Kim[85a], G. Lavizzari[85a,85b],

JHEP10(2026)167

M.T. Lucchini[85a,85b], M. Malberti[85a], S. Malvezzi[85a], A. Massironi[85a], D. Menasce[85a], L. Moroni[85a], M. Paganoni[85a,85b], S. Palluotto[85a,85b], D. Pedrini[85a], A. Perego[85a,85b], G. Pizzati[85a,85b], T. Tabarelli de Fatis[85a,85b], S. Buontempo[86a], C. Di Fraia[86a,86b], F. Fabozzi[86a,86c], L. Favilla[86a,86d], A.O.M. Iorio[86a,86b], L. Lista[86a,86b,ay], P. Paolucci[86a,ac], B. Rossi[86a], P. Azzi[87a], N. Bacchetta[87a,az], D. Bisello[87a,87b], P. Bortignon[87a,87c], G. Bortolato[87a,87b], A.C.M. Bulla[87a,87c], R. Carlin[87a,87b], P. Checchia[87a], T. Dorigo[87a,ba], S. Fantinel[87a], F. Gasparini[87a,87b], U. Gasparini[87a,87b], S. Giorgetti[87a], E. Lusiani[87a], M. Margoni[87a,87b], J. Pazzini[87a,87b], F. Primavera[87a,87b], P. Ronchese[87a,87b], R. Rossin[87a,87b], F. Simonetto[87a,87b], M. Tosi[87a,87b], A. Triossi[87a,87b], S. Ventura[87a], P. Zotto[87a,87b], A. Zucchetta[87a,87b], G. Zumerle[87a,87b], A. Braghieri[88a], S. Calzaferri[88a,88b], P. Montagna[88a,88b], M. Pelliccioni[88a,88b], V. Re[88a], C. Riccardi[88a,88b], P. Salvini[88a], I. Vai[88a,88b], P. Vitulo[88a,88b], S. Ajmal[89a,89b], M.E. Ascioti[89a,89b], G.M. Bilei[89a], C. Carrivale[89a,89b], D. Ciangottini[89a,89b], L. Della Penna[89a,89b], L. Fanò[89a,89b], V. Mariani[89a,89b], M. Menichelli[89a], F. Moscatelli[89a,bb], A. Rossi[89a,89b], A. Santocchia[89a,89b], D. Spiga[89a], T. Tedeschi[89a,89b], C. Aimè[90a,90b], C.A. Alexe[90a,90c], P. Asenov[90a,90b], P. Azzurri[90a], G. Bagliesi[90a], L. Bianchini[90a,90b], T. Boccali[90a], E. Bossini[90a], D. Bruschini[90a,90c], R. Castaldi[90a], F. Cattafesta[90a,90c], M.A. Ciocci[90a,90d], M. Cipriani[90a,90b], R. Dell'Orso[90a], S. Donato[90a,90b], R. Forti[90a,90b], A. Giassi[90a], F. Ligabue[90a,90c], A.C. Marini[90a,90b], A. Messineo[90a,90b], S. Mishra[90a], V.K. Muraleedharan Nair Bindhu[90a,90b], S. Nandan[90a], F. Palla[90a], M. Riggirello[90a,90c], A. Rizzi[90a,90b], G. Rolandi[90a,90c], S. Roy Chowdhury[90a,bc], T. Sarkar[90a], A. Scribano[90a], P. Solanki[90a,90b], P. Spagnolo[90a], F. Tenchini[90a,90b], R. Tenchini[90a], G. Tonelli[90a,90b], N. Turini[90a,90d], F. Vaselli[90a,90c], A. Venturi[90a], P.G. Verdini[90a], P. Akrap[91a,91b], C. Basile[91a,91b], S.C. Behera[91a], F. Cavallari[91a], L. Cunqueiro Mendez[91a,91b], F. De Riggi[91a,91b], D. Del Re[91a,91b], E. Di Marco[91a], M. Diemoz[91a], F. Errico[91a], L. Frosina[91a,91b], R. Gargiulo[91a,91b], B. Harikrishnan[91a,91b], F. Lombardi[91a,91b], E. Longo[91a,91b], L. Martikainen[91a,91b], J. Mijuskovic[91a,91b], G. Organtini[91a,91b], N. Palmeri[91a,91b], R. Paramatti[91a,91b], S. Rahatlou[91a,91b], C. Rovelli[91a], F. Santanastasio[91a,91b], L. Soffi[91a], V. Vladimirov[91a,91b], N. Amapane[92a,92b], R. Arcidiacono[92a,92c], S. Argiro[92a,92b], M. Arneodo[92a,92c], N. Bartosik[92a,92c], R. Bellan[92a,92b], A. Bellora[92a,92b], C. Biino[92a], C. Borca[92a,92b], N. Cartiglia[92a], M. Costa[92a,92b], R. Covarelli[92a,92b], N. Demaria[92a], L. Finco[92a], M. Grippo[92a,92b], B. Kiani[92a,92b], L. Lanteri[92a,92b], F. Legger[92a], F. Luongo[92a,92b], C. Mariotti[92a], S. Maselli[92a], A. Mecca[92a,92b], L. Menzio[92a,92b], P. Meridiani[92a], E. Migliore[92a,92b], M. Monteno[92a], M.M. Obertino[92a,92b], G. Ortona[92a], L. Pacher[92a,92b], N. Pastrone[92a], M. Ruspa[92a,92c], F. Siviero[92a,92b], V. Sola[92a,92b], A. Solano[92a,92b], A. Staiano[92a], C. Tarricone[92a,92b], D. Trocino[92a], G. Umoret[92a,92b], E. Vlasov[92b], R. White[92a,92b], J. Babbar[93a,93b,bc], S. Belforte[93a], V. Candelise[93a,93b], M. Casarsa[93a], F. Cossutti[93a], K. De Leo[93a], G. Della Ricca[93a,93b], R. Delli Gatti[93a,93b], S. Dogra[94], J. Hong[94], J. Kim[94], T. Kim[94], D. Lee[94], H. Lee[94], J. Lee[94], S.W. Lee[94], C.S. Moon[94], Y.D. Oh[94], S. Sekmen[94], B. Tae[94], Y.C. Yang[94], M.S. Kim[95], G. Bak[96], P. Gwak[96], H. Kim[96], D.H. Moon[96], J. Seo[96], E. Asilar[97], F. Carnevali[97], J. Choi[97,bd], T.J. Kim[97], Y. Ryou[97], S. Ha[98], S. Han[98], B.S. Hong[98], J. Kim[98], K. Lee[98], K.S. Lee[98], S. Lee[98],

JHEP10(2026)167

J. Yoo[98], J. Goh[99], J. Shin[99], S. Yang[99], Y. Kang[100], H. Kim[100], Y. Kim[100], B. Ko[100], S. Lee[100], J. Almond[101], J.H. Bhyun[101], J. Choi[101], J. Choi[101], W. Jun[101], H. Kim[101], J. Kim[101], T. Kim[101], Y. Kim[101], Y.W. Kim[101], S. Ko[101], H. Lee[101], J. Lee[101], J. Lee[101], B.H. Oh[101], J. Shin[101], U. Yang[101], I. Yoon[101], W. Jang[102], D.Y. Kang[102], D. Kim[102], S. Kim[102], J.S.H. Lee[102], Y. Lee[102], I. Park[102], Y. Roh[102], I. J. Watson[102], G. Cho[103], K. Hwang[103], B. Kim[103], S. Kim[103], K. Lee[103], H.D. Yoo[103], Y. Lee[104], I. Yu[104], T. Beyrouthy[105], Y. Gharbia[105], F. Alazemi[106], K. Dreimanis[107], O.M. Eberlins[107], A. Gaile[107], C. Munoz Diaz[107], D. Osite[107], G. Pikurs[107], R. Plese[107], A. Potrebko[107], M. Seidel[107], D. Sidiropoulos Kontos[107], N.R. Strautnieks[108], M. Ambrozas[109], A. Juodagalvis[109], S. Nargelas[109], A. Rinkevicius[109], G. Tamulaitis[109], I. Yusuff[110,be], Z. Zolkapli[110], J.F. Benitez[111], A. Castaneda Hernandez[111], A. Cota Rodriguez[111], L.E. Cuevas Picos[111], H.A. Encinas Acosta[111], L.G. Gallegos Maríñez[111], J.A. Murillo Quijada[111], L. Valencia Palomo[111], G. Ayala[112], H. Castilla-Valdez[112], H. Crotte Ledesma[112], R. Lopez-Fernandez[112], J. Mejia Guisao[112], R. Reyes-Almanza[112], A. Sánchez Hernández[112], C. Oropeza Barrera[113], M. Ramírez García[113], D.L. Ramirez Guadarrama[113], I. Bautista[114], F.E. Neri Huerta[114], I. Pedraza[114], H.A. Salazar Ibarguen[114], C. Uribe Estrada[114], I. Bubanja[115], N. Raicevic[115], P.H. Butler[116], A. Ahmad[117], M.I. Asghar[117], A. Awais[117], M.I.M. Awan[117], W.A. Khan[117], V. Avati[118], L. Forthomme[118], L. Grzanka[118], M. Malawski[118], K. Piotrzkowski[118], M. Bluj[119], M. Górski[119], M. Kazana[119], M. Szleper[119], P. Zalewski[119], K. Bunkowski[120], K. Doroba[120], A. Kalinowski[120], M. Konecki[120], J. Krolikowski[120], A. Muhammad[120], P. Fokow[121], K. Pozniak[121], W. Zabolotny[121], M. Araujo[122], D. Bastos[122], C. Beirão Da Cruz E Silva[122], A. Boletti[122], M. Bozzo[122], T. Camporesi[122], G. Da Molin[122], M. Gallinaro[122], J. Hollar[122], N. Leonardo[122], G.B. Marozzo[122], A. Petrilli[122], M. Pisano[122], J. Seixas[122], J. Varela[122], J.W. Wulff[122], P. Adzic[123], L. Markovic[123], P. Milenovic[123], V. Milosevic[123], D. Devetak[124], M. Dordevic[124], J. Milosevic[124], L. Nadderd[124], V. Rekovic[124], M. Stojanovic[124], M. Alcalde Martinez[125], J. Alcaraz Maestre[125], J.A. Brochero Cifuentes[125], M. Cepeda[125], M. Cerrada[125], N. Colino[125], B. De La Cruz[125], A. Delgado Peris[125], A. Escalante Del Valle[125], C. Fernandez Bedoya[125], D. Fernández Del Val[125], J.P. Fernández Ramos[125], J. Flix[125], M.C. Fouz[125], M. Gonzalez Hernandez[125], O. Gonzalez Lopez[125], S. Goy Lopez[125], J.M. Hernandez[125], M.I. Josa[125], J. Llorente Merino[125], O. Manzanilla[125], C. Martin Perez[125], E. Martin Viscasillas[125], D. Moran[125], C.M. Morcillo Perez[125], Á. Navarro Tobar[125], R. Paz Herrera[125], A.M. Pérez-Calero Yzquierdo[125], J. Puerta Pelayo[125], I. Redondo[125], J. Vazquez Escobar[125], J.F. de Trocóniz[126], B. Alvarez Gonzalez[127], J. Ayllon Torresano[127], A. Cardini[127], J. Cuevas[127], J. Del Riego Badas[127], D. Estrada Acevedo[127], J. Fernandez Menendez[127], S. Folgueras[127], I. Gonzalez Caballero[127], P. Leguina[127], M. Obeso Menendez[127], E. Palencia Cortezon[127], J. Prado Pico[127], A. Soto Rodríguez[127], P. Vischia[127], S. Blanco Fernández[128], I.J. Cabrillo[128], A. Calderon[128], J. Duarte Campderros[128], M. Fernandez[128], G. Gomez[128], C. Lasaosa García[128], R. Lopez Ruiz[128], C. Martinez Rivero[128], P. Martinez Ruiz del Arbol[128], F. Matorras[128], P. Matorras Cuevas[128], E. Navarrete Ramos[128], J. Piedra Gomez[128],

JHEP10(2026)167

C. Quintana San Emeterio[128], L. Scodellaro[128], I. Vila[128], R. Vilar Cortabitarte[128], J.M. Vizan Garcia[128], D.C.W. Dhammage[129], B. Kailasapathy[129,bf], W.G. Dharmaratna[130,bg], K. Liyanage[130], N. Perera[130], T. Bevilacqua[131,bh], L. Caminada[131,bh], W. Erdmann[131], R. Horisberger[131], Q. Ingram[131], H.C. Kaestli[131], D. Kotlinski[131], C. Lange[131], U. Langenegger[131], A. Nigamova[131], L. Noehte[131,bh], T. Rohe[131], A. Samalan[131], T.K. Aarrestad[132], M. Backhaus[132], G. Bonomelli[132], C. Cazzaniga[132], K. Datta[132], P. De Bryas Dexmiers D'Archiacchiac[132,j], A. De Cosa[132], G. Dissertori[132], M. Dittmar[132], M. Donegà[132], F. Glessgen[132], C. Grab[132], N. Härringer[132], T.G. Harte[132], W. Lustermann[132], M. Malucchi[132], R.A. Manzoni[132], L. Marchese[132], A. Mascellani[132,j], F. Nessi-Tedaldi[132], F. Pauss[132], B. Ristic[132], R. Seidita[132], J. Steggemann[132,j], A. Tarabini[132], D. Valsecchi[132], R. Wallny[132], C. Amsler[133,bi], P. Bärtschi[133], F. Bilandzija[133], M.F. Canelli[133], G. Celotto[133], V. Guglielmi[133], A. Jofrehei[133], B. Kilminster[133], T.H. Kwok[133], S. Leontsinis[133], V. Lukashenko[133], A. Macchiolo[133], F. Meng[133], M. Missiroli[133], J. Motta[133], P. Robmann[133], E. Shokr[133], F. Stäger[133], R. Tramontano[133], P. Viscone[133], D. Bhowmik[134], C.M. Kuo[134], P.K. Rout[134], S. Taj[134], P.C. Tiwari[134,al], L. Ceard[135], K.F. Chen[135], Z.g. Chen[135], A. De Iorio[135], G.W.S. Hou[135], T.h. Hsu[135], Y.w. Kao[135], S. Karmakar[135], G. Kole[135], Y.y. Li[135], R.S. Lu[135], E. Paganis[135], X.f. Su[135], J. Thomas-Wilsker[135], L.s. Tsai[135], D. Tsionou[135], H.y. Wu[135], E. Yazgan[135], C. Asawatangtrakuldee[136], N. Srimanobhas[136], Y. Maghrbi[137], D. Agyel[138], F. Dolek[138], I. Dumanoglu[138,bj], Y. Guler[138,bk], E. Gurpinar Guler[138,bk], C. Isik[138], O. Kara[138,bl], A. Kayis Topaksu[138], Y. Komurcu[138], G. Onengut[138], K. Ozdemir[138,bm], B. Tali[138,bn], U.G. Tok[138], E. Uslan[138], I.S. Zorbakir[138], S. Sen[139], M. Yalvac[140,bo], B. Akgun[141], I.O. Atakisi[141,bp], E. Gülmez[141], M. Kaya[141,bq], O. Kaya[141,br], M.A. Sarkisla[141,bs], S. Tekten[141,bt], D. Boncukcu[142], A. Cakir[142], K. Cankocak[142,bj,bu], B. Hacisahinoglu[143], I. Hos[143,bv], B. Kaynak[143], S. Ozkorucuklu[143], O. Potok[143], H. Sert[143], C. Simsek[143], C. Zorbilmez[143], S. Cerci[144], C. Dozen[144,bw], B. Isildak[144], E. Simsek[144], D. Sunar Cerci[144], T. Yetkin[144,bw], A. Boyaryntsev[145], O. Dadazhanova[145], B. Grynyov[145], L. Levchuk[146], J.J. Brooke[147], A. Bundock[147], F.J.J. Bury[147], E. Clement[147], D. Cussans[147], D. Dharmender[147], H. Flacher[147], J. Goldstein[147], H.F. Heath[147], M.l. Holmberg[147], L. Kreczko[147], S. Paramesvaran[147], L. Robertshaw[147], M.S. Sanjrani[147,ao], J. Segal[147], V.J. Smith[147], A. Ball[148], K.W. Bell[148], A. Belyaev[148,bx], C. Brew[148], R.M. Brown[148], D.J. Cockerill[148], A. Elliot[148], K.V. Ellis[148], J. Gajownik[148], K. Harder[148], S. Harper[148], J. Linacre[148], K. Manolopoulos[148], M. Moallemi[148], D.M. Newbold[148], E. Olaiya[148], D. Petyt[148], T. Reis[148], A.R. Sahasransu[148], G. Salvi[148], T. Schuh[148], C. Shepherd-Themistocleous[148], I.R. Tomalin[148], K.C. Whalen[148], T. Williams[148], I. Andreou[149], R. Bainbridge[149], P. Bloch[149], O. Buchmuller[149], C.A. Carrillo Montoya[149], D. Colling[149], I. Das[149], P. Dauncey[149], G. Davies[149], M. Della Negra[149], S. Fayer[149], G. Fedi[149], G. Hall[149], H.R. Hoorani[149], A. Howard[149], G. Iles[149], C.R. Knight[149], P. Krueper[149], J. Langford[149], K.H. Law[149], J. León Holgado[149], L. Lyons[149], A.M. Magnan[149], B. Maier[149], S. Mallios[149], A. Mastronikolis[149], M. Mieskolainen[149], J. Nash[149,by], M. Pesaresi[149], P.B. Pradeep[149], B.C. Radburn-Smith[149], A. Richards[149], A. Rose[149], L. Russell[149], K. Savva[149], C. Seez[149], R. Shukla[149], A. Tapper[149],

JHEP10(2026)167

K. Uchida[149], G.P. Uttley[149], T. Virdee[149,ac], M. Vojinovic[149], N. Wardle[149], D. Winterbottom[149], J. Cole[150], A. Khan[150], P. Kyberd[150], I. Reid[150], B. Bam[151], A. Buchot Perraguin[151], S. Campbell[151], R. Chudasama[151], S. Cooper[151], C. Crovella[151], G. Fidalgo[151], S.V. Gleyzer[151], A. Khukhunaishvili[151], K. Matchev[151], E. Pearson[151], P. Rumerio[151,bz], E. Usai[151], R. Yi[151], S. Abbott[152], S. Baradia[152], B. Barton[152], R. Breedon[152], H. Cai[152], M. Calderon De La Barca Sanchez[152], E. Cannaert[152], M. Chertok[152], M. Citron[152], J. Conway[152], P.T. Cox[152], F. Eble[152], R. Erbacher[152], O. Kukral[152], G. Mocellin[152], S. Ostrom[152], I. Salazar Segovia[152], J.S. Tafoya Vargas[152], W. Wei[152], S. Yoo[152], A. Aportela[153], A. Arora[153], J.G. Branson[153], S. Cittolin[153], S. Cooperstein[153], B. D'Anzi[153], D. Diaz[153], J. Duarte[153], L. Giannini[153], Y. Gu[153], J. Guiang[153], V. Krutelyov[153], R. Lee[153], J. Letts[153], H. Li[153], M. Masciovecchio[153], F. Mokhtar[153], S. Mukherjee[153], M. Pieri[153], D. Primosch[153], M. Quinnan[153], V. Sharma[153], M. Tadel[153], E. Vourliotis[153], F. Würthwein[153], A. Yagil[153], Z. Zhao[153], K. Adamidis[154], M. Bachtis[154], D. Campos[154], R. Cousins[154], S. Crossley[154], G. Flores Avila[154], J. Hauser[154], M. Ignatenko[154], M.A. Iqbal[154], T. Lam[154], Y.f. Lo[154], E. Manca[154], A. Nunez Del Prado[154], D. Saltzberg[154], V. Valuev[154], A. Albert[155], S. Bhattacharya[155], A. Bornheim[155], O. Cerri[155], R. Kansal[155], J. Mao[155], H.B. Newman[155], G. Reales Gutiérrez[155], T. Sievert[155], M. Spiropulu[155], J.R. Vlimant[155], R.A. Wynne[155], S. Xie[155], R. Clare[156], J.W. Gary[156], G. Hanson[156], A. Barzdukas[157], L. Brennan[157], C. Campagnari[157], S. Carron Montero[157,ca], K. Downham[157], C. Grieco[157], M.M. Hussain[157], J. Incandela[157], M.W.K. Lai[157], A.J. Li[157], P. Masterson[157], J. Richman[157], S.N. Santpur[157], R. Schmitz[157], D. Stuart[157], T.Á. Vámi[157], X. Yan[157], D. Zhang[157], J.P. Cumalat[158], W.T. Ford[158], A. Hart[158], S. Kwan[158], J. Pearkes[158], C. Savard[158], N. Schonbeck[158], K. Stenson[158], K. Ulmer[158], S.R. Wagner[158], N. Zipper[158], D. Zuolo[158], R. Bartek[159], A. Dominguez[159], S. Raj[159], B. Sahu[159,ak], A.E. Simsek[159], S.S. Yu[159], C. Aruta[160], P. Avery[160], D. Bourilkov[160], P. Chang[160], V. Cherepanov[160], R.D. Field[160], C. Huh[160], E. Koenig[160], M. Kolosova[160], J. Konigsberg[160], A. Korytov[160], G. Mitselmakher[160], K. Mohrman[160], A. Muthirakalayil Madhu[160], N. Rawal[160], S. Rosenzweig[160], V. Sulimov[160], Y. Takahashi[160], J. Wang[160], B. Alsufyani[161], S. Butalla[161], S. Das[161], M. Hohlmann[161], M. Lavinsky[161], E. Yanes[161], T. Adams[162], A. Al Kadhim[162], A. Askew[162], S. Bower[162], R. Goff[162], R. Hashmi[162], A. Hassani[162], R.S. Kim[162], T. Kolberg[162], G. Martinez[162], M. Mazza[162], H. Prosper[162], P.R. Prova[162], R. Yohay[162], M. Albrow[163], M. Alyari[163], O. Amram[163], G. Apollinari[163], A. Apresyan[163], L.A. Bauerdick[163], D. Berry[163], J. Berryhill[163], P.C. Bhat[163], K. Burkett[163], J.N. Butler[163], A. Canepa[163], G.B. Cerati[163], H. Cheung[163], F. Chlebana[163], C. Cosby[163], G. Cummings[163], I. Dutta[163], V.D. Elvira[163], J. Freeman[163], A. Gandrakota[163], Z. Gecse[163], L. Gray[163], D. Green[163], A. Grummer[163], S. Grünendahl[163], D. Guerrero[163], O. Gutsche[163], R.M. Harris[163], J. Hirschauer[163], V. Innocente[163], B. Jayatilaka[163], S. Jindariani[163], M. Johnson[163], U. Joshi[163], B. Klima[163], S. Lammel[163], C. Lee[163], D. Lincoln[163], R. Lipton[163], T. Liu[163], K. Maeshima[163], D. Mason[163], P. McBride[163], P. Merkel[163], S. Mrenna[163], S. Nahn[163], J. Ngadiuba[163], D. Noonan[163], S. Norberg[163], V. Papadimitriou[163], N. Pastika[163], K. Pedro[163], C. Pena[163,cb], C.E. Perez Lara[163],

JHEP10(2026)167

V. Perovic[163], F. Ravera[163], A. Reinsvold Hall[163,cc], L. Ristori[163], M. Safdari[163], E. Sexton-Kennedy[163], E. Smith[163], N. Smith[163], A. Soha[163], L. Spiegel[163], S. Stoynev[163], J. Strait[163], L. Taylor[163], S. Tkaczyk[163], N.V. Tran[163], L. Uplegger[163], E.W. Vaandering[163], C. Wang[163], I. Zoi[163], M.R. Adams[164], N. Barnett[164], A. Baty[164], C. Bennett[164], R. Cavanaugh[164], R. Escobar Franco[164], O. Evdokimov[164], C.E. Gerber[164], H. Gupta[164], M. Hawksworth[164], A. Hingrajiya[164], D.J. Hofman[164], Z. Huang[164], J.h. Lee[164], C. Mills[164], S. Nanda[164], G. Nigmatkulov[164], B. Ozek[164], T. Phan[164], D. Pilipovic[164], R. Pradhan[164], E. Prifti[164], P. Roy[164], T. Roy[164], D. Shekar[164], N. Singh[164], A. Thielen[164], M. Tonjes[164], N. Varelas[164], M.A. Wadud[164], J. Yoo[164], S. Dittmer[165], K.A. Hahn[165], M. Mcginnis[165], Y. Miao[165], D.G. Monk[165], M.H. Schmitt[165], A. Taliercio[165], M. Velasco[165], J. Wang[165], N. Parashar[166], A. Pathak[166], E. Shumka[166], G. Agarwal[167], R. Band[167], R. Bucci[167], S. Castells[167], A. Das[167], A. Datta[167], A. Ehnis[167], R. Goldouzian[167], M. Hildreth[167], K. Hurtado Anampa[167], T. Ivanov[167], C. Jessop[167], A. Karneyeu[167], K. Lannon[167], J. Lawrence[167], N. Loukas[167], D. Lutton[167], J. Mariano[167], N. Marinelli[167], T. McCauley[167], C. Mcgrady[167], C. Moore[167], Y. Musienko[167,cd], H. Nelson[167], M. Osherson[167], A. Piccinelli[167], R. Ruchti[167], A. Townsend[167], Y. Wan[167], M. Wayne[167], H. Yockey[167], S. Chandra[168], A. Gu[168], L. Gutay[168], M. Huwiler[168], M. Jones[168], A.W. Jung[168], D. Kondratyev[168], J. Li[168], M. Liu[168], G. Negro[168], N. Neumeister[168], G. Paspalaki[168], S. Piperov[168], N.R. Saha[168], J.F. Schulte[168], F. Wang[168], A. Wildridge[168], W. Xie[168], Y. Yao[168], Y. Zhong[168], M. Alhusseini[169], D. Blend[169], K. Dilsiz[169,ce], O.K. Köseyan[169], A. Mestvirishvili[169,cf], O. Neogi[169], H. Ogul[169,cg], Y. Onel[169], A. Penzo[169], C. Snyder[169], E. Tiras[169,ch], A. Abreu[170], L.F. Alcerro Alcerro[170], J. Anguiano[170], S. Arteaga Escatel[170], P. Baringer[170], A. Bean[170], R. Bhattacharya[170], Z. Flowers[170], D. Grove[170], J. King[170], G. Krintiras[170], M. Lazarovits[170], C. Le Mahieu[170], J. Marquez[170], M. Murray[170], M. Nickel[170], S. Popescu[170,ci], C. Rogan[170], C. Royon[170], S. Rudrabhatla[170], S. Sanders[170], C. Smith[170], G. Wilson[170], B. Allmond[171], N. Islam[171], A. Ivanov[171], K. Kaadze[171], Y. Maravin[171], J. Natoli[171], G.G. Reddy[171], D. Roy[171], G. Sorrentino[171], B. Blumenfeld[172], J. Davis[172], A. Gritsan[172], L. Kang[172], S. Kyriacou[172], P. Maksimovic[172], M. Roguljic[172], S. Sekhar[172], M.V. Srivastav[172], M. Swartz[172], D. Baden[173], A. Belloni[173], J. Bistany-riebman[173], S.C. Eno[173], N.J. Hadley[173], S. Jabeen[173], R.G. Kellogg[173], T. Koeth[173], B. Kronheim[173], S. Lascio[173], P. Major[173], A. Mignerey[173], C. Palmer[173], C. Papageorgakis[173], M.M. Paranjpe[173], E. Popova[173,cj], A. Shevelev[173], L. Zhang[173], S. Cholak[174], G. De Castro[174], Z. Demiragli[174], C. Erice[174], C. Fangmeier[174], C. Fernandez Madrazo[174], J. Fulcher[174], F. Golf[174], S. Jeon[174], J. O'Cain[174], I. Reed[174], J. Rohlf[174], K. Salyer[174], D. Sperka[174], D. Spitzbart[174], I. Suarez[174], A. Tsatsos[174], E. Wurtz[174], A.G. Zecchinelli[174], A. Aarif[175], G. Alverson[175], E. Barberis[175], J. Bonilla[175], B. Bylsma[175], M. Campana[175], J. Dervan[175], Y. Haddad[175], Y. Han[175], I. Israr[175], A. Krishna[175], M. Lu[175], N. Manganelli[175], R. Mccarthy[175], D.M. Morse[175], T. Orimoto[175], L. Skinnari[175], C.S. Thoreson[175], E. Tsai[175], D. Wood[175], C. Baldenegro Barrera[176], H. Bossi[176], S. Bright-Thonney[176], I.A. Cali[176], Y.c. Chen[176], P.c. Chou[176], M. D'Alfonso[176], J. Eysermans[176], C. Freer[176], G. Gomez Ceballos[176], M. Goncharov[176], G. Grosso[176], P. Harris[176], D. Hoang[176],

JHEP10(2026)167

G.M. Innocenti[176], K. Ivanov[176], D. Kovalskyi[176], J. Krupa[176], L. Lavezzo[176], Y.J. Lee[176], K. Long[176], C. Mcginn[176], A. Novak[176], M.I. Park[176], C. Paus[176], C. Reissel[176], C. Roland[176], G. Roland[176], S. Rothman[176], T.a. Sheng[176], G. Stephans[176], D. Walter[176], J. Wang[176], Z. Wang[176], B. Wyslouch[176], T. Yang[176], S. Bhattacharya[177], P.E. Karchin[177], A. Alpana[178], B. Crossman[178], W.J. Jackson[178], C. Kapsiak[178], M. Krohn[178], D. Mahon[178], J. Mans[178], B. Marzocchi[178], R. Rusack[178], O. Sancar[178], R. Saradhy[178], N. Strobbe[178], J.M. Hogan[179], K. Bloom[180], D.R. Claes[180], G. Haza[180], J. Hossain[180], C. Joo[180], I. Kravchenko[180], K.H.M. Kwok[180], A. Rohilla[180], J.E. Siado[180], W. Tabb[180], A. Vagnerini[180], A. Wightman[180], F. Yan[180], B. Chiarito[181], J.P. Chou[181], S.V. Clark[181], S. Donnelly[181], D. Gadkari[181], Y. Gershtein[181], E. Halkiadakis[181], C. Houghton[181], D. Jaroslawski[181], A. Kobert[181], I. Laflotte[181], A. Lath[181], J. Martins[181], M. Perez Prada[181], B. Rand[181], J. Reichert[181], P. Saha[181], S. Salur[181], S. Schnetzer[181], S. Somalwar[181], R. Stone[181], S.A. Thayil[181], S. Thomas[181], J. Vora[181], H. Bouchamaoui[182], G. Dezoort[182], P. Elmer[182], A. Frankenthal[182], M. Galli[182], B. Greenberg[182], N. Haubrich[182], K. Kennedy[182], G. Kopp[182], Y. Lai[182], D. Lange[182], A. Loeliger[182], D. Marlow[182], I. Ojalvo[182], J. Olsen[182], F. Simpson[182], D. Stickland[182], C. Tully[182], H. Bandyopadhyay[183], L. Hay[183], H.w. Hsia[183], I. Iashvili[183], A. Kalogeropoulos[183], A. Kharchilava[183], A. Mandal[183], M. Morris[183], D. Nguyen[183], S. Rappoccio[183], H. Rejeb Sfar[183], A. Williams[183], D. Yu[183], J. Alexander[184], X. Chen[184], J. Dickinson[184], A. Duquette[184], J. Fan[184], X. Fan[184], J. Grassi[184], S. Hogan[184], P. Kotamnives[184], J. Monroy[184], G. Niendorf[184], M. Oshiro[184], J.R. Patterson[184], A. Ryd[184], J. Thom[184], P. Wittich[184], R. Zou[184], L. Zygala[184], O. Bessidskaia Bylund[185], A. Bodek[185], P. de Barbaro[185], R. Demina[185], A. Garcia-Bellido[185], H.S. Hare[185], O. Hindrichs[185], N. Parmar[185], P. Parygin[185,cj], H. Seo[185], R. Taus[185], M. Carrigan[186], R. De Los Santos[186], L.S. Durkin[186], C. Hill[186], M. Joyce[186], D.A. Wenzl[186], B.L. Winer[186], B. Yates[186], J. Alison[187], S. An[187], M. Cremonesi[187], V. Dutta[187], E.Y. Ertorer[187], T. Ferguson[187], T.A. Gómez Espinosa[187], A. Harilal[187], A. Kallil Tharayil[187], M. Kanemura[187], C. Liu[187], M. Marchegiani[187], P. Meiring[187], S. Murthy[187], P. Palit[187], K. Park[187], M. Paulini[187], A. Roberts[187], A. Sanchez[187], W. Terrill[187], S. Malik[188], R. Sharma[188], G. Barone[189], G. Benelli[189], D. Cutts[189], S. Ellis[189], L. Gouskos[189], M. Hadley[189], U. Heintz[189], K.W. Ho[189], T. Kwon[189], L. Lambrecht[189], G. Landsberg[189], K.T. Lau[189], J. Luo[189], S. Mondal[189], J. Roloff[189], T. Russell[189], S. Sagir[189,ck], X. Shen[189], M. Stamenkovic[189], N. Venkatasubramanian[189], D. Ally[190], A.G. Delannoy[190], S. Fiorendi[190], J. Harris[190], T. Holmes[190], A.R. Kanuganti[190], N. Karunarathna[190], J. Lawless[190], L. Lee[190], E. Nibigira[190], B. Skipworth[190], S. Spanier[190], E. Appelt[191], Y. Chen[191], S. Greene[191], A. Gurrola[191], W. Johns[191], R. Kunnawalkam Elayavalli[191], A. Melo[191], D. Rathjens[191], F. Romeo[191], P. Sheldon[191], S. Tuo[191], J. Velkovska[191], J. Viinikainen[191], J. Zhang[191], D. Aebi[192], M. Ahmad[192], T. Akhter[192], K. Androsov[192], A. Basnet[192], A. Bolshov[192], O. Bouhali[192,cl], A. Cagnotta[192], V. D'Amante[192], R. Eusebi[192], P. Flanagan[192], J. Gilmore[192], Y. Guo[192], T. Kamon[192], S. Luo[192], R. Mueller[192], A. Safonov[192], D. Acosta[193], A. Agrawal[193], C. Arbour[193], T. Carnahan[193], P. Das[193], K.M. Ecklund[193], F.J. Geurts[193], T. Huang[193], I. Krommydas[193], N. Lewis[193], W. Li[193],

JHEP10(2026)167

J. Lin[193], O. Miguel Colin[193], B.P. Padley[193], R. Redjimi[193], J. Rotter[193], C. Vico Villalba[193], M. Wulansatiti[193], E. Yigitbasi[193], Y. Zhang[193], N. Akchurin[194], J. Damgov[194], Y. Feng[194], N. Gogate[194], W. Jin[194], Y. Kazhykarim[194], K. Lamichhane[194], S.W. Lee[194], C. Madrid[194], A. Mankel[194], T. Peltola[194], I. Volobouev[194], S. Abdullin[195], A. Brinkerhoff[195], E. Collins[195], M.R. Darwish[195], J. Dittmann[195], K. Hatakeyama[195], V. Hegde[195], J. Hiltbrand[195], B. McMaster[195], J. Samudio[195], S. Sawant[195], C. Sutantawibul[195], J. Wilson[195], B. Cardwell[196], H. Chung[196], B. Cox[196], J. Hakala[196], G. Hamilton Ilha Machado[196], R. Hirosky[196], M. Jose[196], A. Ledovskoy[196], C. Mantilla[196], C. Neu[196], C. Ramón Álvarez[196], Z. Wu[196], A. Aravind[197], S. Banerjee[197], K. Black[197], T. Bose[197], E. Chavez[197], S. Dasu[197], P. Everaerts[197], C. Galloni[197], H. He[197], M. Herndon[197], A. Herve[197], C.K. Koraka[197], S. Lomte[197], R. Loveless[197], A. Mallampalli[197], A. Mohammadi[197], S. Mondal[197], T. Nelson[197], G. Parida[197], L. Pétré[197], D. Pinna[197], A. Savin[197], V. Shang[197], V. Sharma[197], W.H. Smith[197], D. Teague[197], H.F. Tsoi[197], W. Vetens[197], A. Warden[197], S. Afanasiev[198], V. Alexakhin[198], Y. Andreev[198], T. Aushev[198], D. Budkouski[198], R. Chistov[198], M. Danilov[198], T. Dimova[198], A. Ershov[198], S. Gninenko[198], I. Gorbunov[198], A. Gribushin[198], A. Kamenev[198], V. Karjavine[198], M. Kirsanov[198], V. Klyukhin[198], O. Kodolova[198,cm], V. Korenkov[198], I. Korsakov[198], A. Kozyrev[198], N. Krasnikov[198], A. Lanev[198], A. Malakhov[198], V. Matveev[198], A. Nikitenko[198,cn,cm], V. Palichik[198], V. Perelygin[198], S. Petrushanko[198], O. Radchenko[198], M. Savina[198], V. Shalaev[198], S. Shmatov[198], S. Shulha[198], Y. Skovpen[198], K. Slizhevskiy[198], V. Smirnov[198], O. Teryaev[198], I. Tlisova[198], A. Toropin[198], N. Voytishin[198], A. Zarubin[198], I. Zhizhin[198], E. Boos[199], V. Bunichev[199], M. Dubinin[199,cb], L. Dudko[199], V. Kim[199,cd], V. Murzin[199], V. Oreshkin[199], V. Savrin[199], A. Snigirev[199], D. Sosnov[199]

[1] *Yerevan Physics Institute, Yerevan, Armenia*
[2] *Institut für Hochenergiephysik, Vienna, Austria*
[3] *Universiteit Antwerpen, Antwerpen, Belgium*
[4] *Vrije Universiteit Brussel, Brussel, Belgium*
[5] *Université Libre de Bruxelles, Bruxelles, Belgium*
[6] *Ghent University, Ghent, Belgium*
[7] *Université Catholique de Louvain, Louvain-la-Neuve, Belgium*
[8] *Centro Brasileiro de Pesquisas Fisicas, Rio de Janeiro, Brazil*
[9] *Universidade do Estado do Rio de Janeiro, Rio de Janeiro, Brazil*
[10] *Universidade Estadual Paulista (a), Universidade Federal do ABC (b), São Paulo, Brazil*
[11] *Institute for Nuclear Research and Nuclear Energy, Bulgarian Academy of Sciences, Sofia, Bulgaria*
[12] *University of Sofia, Sofia, Bulgaria*
[13] *CERN, European Organization for Nuclear Research, Geneva, Switzerland*
[14] *Instituto de Alta Investigación, Universidad de Tarapacá, Arica, Chile*
[15] *Universidad Técnica Federico Santa María, Valparaiso, Chile*
[16] *Beihang University, Beijing, China*
[17] *Department of Physics, Tsinghua University, Beijing, China*
[18] *Institute of High Energy Physics, Beijing, China*
[19] *State Key Laboratory of Nuclear Physics and Technology, Peking University, Beijing, China*
[20] *State Key Laboratory of Nuclear Physics and Technology, Institute of Quantum Matter, South China Normal University, Guangzhou, China, Guangzhou, China*
[21] *Sun Yat-Sen University, Guangzhou, China*
[22] *University of Science and Technology of China, Hefei, China*

JHEP10(2026)167

[23] Nanjing Normal University, Nanjing, China
[24] Institute of Modern Physics and Key Laboratory of Nuclear Physics and Ion-beam Application (MOE) — Fudan University, Shanghai, China
[25] Zhejiang University — Department of Physics, Zhejiang, China
[26] Universidad de Los Andes, Bogota, Colombia
[27] Universidad de Antioquia, Medellin, Colombia
[28] University of Split, Faculty of Electrical Engineering, Mechanical Engineering and Naval Architecture, Split, Croatia
[29] University of Split, Faculty of Science, Split, Croatia
[30] Institute Rudjer Boskovic, Zagreb, Croatia
[31] University of Cyprus, Nicosia, Cyprus
[32] Charles University, Prague, Czech Republic
[33] Escuela Politecnica Nacional, Quito, Ecuador
[34] Universidad San Francisco de Quito, Quito, Ecuador
[35] Academy of Scientific Research and Technology of the Arab Republic of Egypt, Egyptian Network of High Energy Physics, Cairo, Egypt
[36] Center for High Energy Physics (CHEP-FU), Fayoum University, El-Fayoum, Egypt
[37] National Institute of Chemical Physics and Biophysics, Tallinn, Estonia
[38] Department of Physics, University of Helsinki, Helsinki, Finland
[39] Helsinki Institute of Physics, Helsinki, Finland
[40] Lappeenranta-Lahti University of Technology, Lappeenranta, Finland
[41] IRFU, CEA, Université Paris-Saclay, Gif-sur-Yvette, France
[42] Laboratoire Leprince-Ringuet, CNRS/IN2P3, Ecole Polytechnique, Institut Polytechnique de Paris, Palaiseau, France
[43] Institut Pluridisciplinaire Hubert Curien (IPHC), Université de Strasbourg, CNRS/IN2P3, Strasbourg, France
[44] Centre de Calcul de l'Institut National de Physique Nucleaire et de Physique des Particules, CNRS/IN2P3, Villeurbanne, France
[45] Institut de Physique des 2 Infinis de Lyon (IP2I), Villeurbanne, France
[46] Georgian Technical University, Tbilisi, Georgia
[47] RWTH Aachen University, I. Physikalisches Institut, Aachen, Germany
[48] RWTH Aachen University, III. Physikalisches Institut A, Aachen, Germany
[49] RWTH Aachen University, III. Physikalisches Institut B, Aachen, Germany
[50] Deutsches Elektronen-Synchrotron, Hamburg, Germany
[51] University of Hamburg, Hamburg, Germany
[52] Institut für Experimentelle Teilchenphysik, Karlsruhe, Germany
[53] Institute of Nuclear and Particle Physics (INPP), NCSR Demokritos, Aghia Paraskevi, Greece
[54] National and Kapodistrian University of Athens, Athens, Greece
[55] National Technical University of Athens, Athens, Greece
[56] University of Ioánnina, Ioánnina, Greece
[57] HUN-REN Wigner Research Centre for Physics, Budapest, Hungary
[58] MTA-ELTE Lendület CMS Particle and Nuclear Physics Group, Eötvös Loránd University, Budapest, Hungary
[59] Faculty of Informatics, University of Debrecen, Debrecen, Hungary, Debrecen, Hungary
[60] HUN-REN ATOMKI — Institute of Nuclear Research, Debrecen, Hungary
[61] Karoly Robert Campus, MATE Institute of Technology, Gyongyos, Hungary
[62] Indian Institute of Technology Bhubaneswar, Bhubaneswar, India
[63] Panjab University, Chandigarh, India
[64] University of Delhi, Delhi, India
[65] Indian Institute of Technology Mandi (IIT-Mandi), Himachal Pradesh, India
[66] University of Hyderabad, Hyderabad, India
[67] Indian Institute of Technology Kanpur, Kanpur, India
[68] Saha Institute of Nuclear Physics, HBNI, Kolkata, India

JHEP10(2026)167

[69] Indian Institute of Technology Madras, Madras, India
[70] Indian lnstitute of Science Education and Research Mohali, Mohali, India
[71] Tata Institute of Fundamental Research-A, Mumbai, India
[72] Tata Institute of Fundamental Research-B, Mumbai, India
[73] National Institute of Science Education and Research, Jatni, Khorda, Odisha 752050, India Homi Bhabha National Institute, Training School Complex, Anushakti Nagar, Mumbai 400094, India, Odisha, India
[74] Indian Institute of Science Education and Research (IISER), Pune, India
[75] Indian Institute of Technology Hyderabad, Telangana, India
[76] Isfahan University of Technology, Isfahan, Iran
[77] Institute for Research in Fundamental Sciences (IPM), Tehran, Iran
[78] University College Dublin, Dublin, Ireland
[79a] INFN Sezione di Bari, Bari, Italy
[79b] Università di Bari, Bari, Italy
[79c] Politecnico di Bari, Bari, Italy
[80a] INFN Sezione di Bologna, Bologna, Italy
[80b] Università di Bologna, Bologna, Italy
[81a] INFN Sezione di Catania, Catania, Italy
[81b] Università di Catania, Catania, Italy
[82a] INFN Sezione di Firenze, Firenze, Italy
[82b] Università di Firenze, Firenze, Italy
[83] INFN Laboratori Nazionali di Frascati, Frascati, Italy
[84a] INFN Sezione di Genova, Genova, Italy
[84b] Università di Genova, Genova, Italy
[85a] INFN Sezione di Milano-Bicocca, Milano-Bicocca, Italy
[85b] Università di Milano-Bicocca, Milano, Milano-Bicocca, Italy
[86a] INFN Sezione di Napoli, Napoli, Italy
[86b] Università di Napoli 'Federico II', Napoli, Italy
[86c] Università della Basilicata (Potenza), Napoli, Italy
[86d] Scuola Superiore Meridionale (SSM), Napoli, Italy
[87a] INFN Sezione di Padova, Padova, Italy
[87b] Università di Padova, Padova, Italy
[87c] Universita degli Studi di Cagliari, Padova, Italy
[88a] INFN Sezione di Pavia, Pavia, Italy
[88b] Università di Pavia, Pavia, Italy
[89a] INFN Sezione di Perugia, Perugia, Italy
[89b] Università di Perugia, Perugia, Italy
[90a] INFN Sezione di Pisa, Pisa, Italy
[90b] Università di Pisa, Pisa, Italy
[90c] Scuola Normale Superiore di Pisa, Pisa, Italy
[90d] Università di Siena, Pisa, Italy
[91a] INFN Sezione di Roma, Roma, Italy
[91b] Sapienza Università di Roma, Roma, Italy
[92a] INFN Sezione di Torino, Torino, Italy
[92b] Università di Torino, Torino, Italy
[92c] Università del Piemonte Orientale (Novara), Torino, Italy
[93a] INFN Sezione di Trieste, Trieste, Italy
[93b] Università di Trieste, Trieste, Italy
[94] Kyungpook National University, Daegu, Korea
[95] Department of Mathematics and Physics — Gangneung-Wonju National University, Gangneung, Korea
[96] Chonnam National University, Institute for Universe and Elementary Particles, Kwangju, Korea
[97] Hanyang University, Seoul, Korea
[98] Korea University, Seoul, Korea
[99] Kyung Hee University, Department of Physics, Seoul, Korea

JHEP10(2026)167

[100] *Sejong University, Seoul, Korea*
[101] *Seoul National University, Seoul, Korea*
[102] *University of Seoul, Seoul, Korea*
[103] *Yonsei University, Department of Physics, Seoul, Korea*
[104] *Sungkyunkwan University, Suwon, Korea*
[105] *College of Engineering and Technology, American University of the Middle East (AUM), Dasman, Kuwait*
[106] *Kuwait University — College of Science — Department of Physics, Safat, Kuwait*
[107] *Riga Technical University, Riga, Latvia*
[108] *University of Latvia (LU), Riga, Latvia*
[109] *Vilnius University, Vilnius, Lithuania*
[110] *National Centre for Particle Physics, Universiti Malaya, Kuala Lumpur, Malaysia*
[111] *University of Sonora (UNISON), Hermosillo, Mexico*
[112] *Centro de Investigacion y de Estudios Avanzados del IPN, Mexico City, Mexico*
[113] *Universidad Iberoamericana, Mexico City, Mexico*
[114] *Benemerita Universidad Autonoma de Puebla, Puebla, Mexico*
[115] *University of Montenegro, Podgorica, Montenegro*
[116] *University of Canterbury, Christchurch, New Zealand*
[117] *National Centre for Physics, Quaid-I-Azam University, Islamabad, Pakistan*
[118] *AGH University of Krakow, Krakow, Poland*
[119] *National Centre for Nuclear Research, Swierk, Poland*
[120] *Institute of Experimental Physics, Faculty of Physics, University of Warsaw, Warsaw, Poland*
[121] *Warsaw University of Technology, Warsaw, Poland*
[122] *Laboratório de Instrumentação e Física Experimental de Partículas, Lisboa, Portugal*
[123] *Faculty of Physics, University of Belgrade, Belgrade, Serbia*
[124] *Vinca Institute of Nuclear Science, Belgrade, Serbia*
[125] *Centro de Investigaciones Energéticas Medioambientales y Tecnológicas (CIEMAT), Madrid, Spain*
[126] *Universidad Autónoma de Madrid, Madrid, Spain*
[127] *Universidad de Oviedo, Instituto Universitario de Ciencias y Tecnologías Espaciales de Asturias (ICTEA), Oviedo, Spain*
[128] *Instituto de Física de Cantabria (IFCA), CSIC-Universidad de Cantabria, Santander, Spain*
[129] *University of Colombo, Colombo, Sri Lanka*
[130] *University of Ruhuna, Department of Physics, Matara, Sri Lanka*
[131] *PSI Center for Neutron and Muon Sciences, Villigen, Switzerland*
[132] *ETH Zurich — Institute for Particle Physics and Astrophysics (IPA), Zurich, Switzerland*
[133] *Universität Zürich, Zurich, Switzerland*
[134] *National Central University, Chung-Li, Taiwan*
[135] *National Taiwan University (NTU), Taipei, Taiwan*
[136] *High Energy Physics Research Unit, Department of Physics, Faculty of Science, Chulalongkorn University, Bangkok, Thailand*
[137] *Tunis El Manar University, Tunis, Tunisia*
[138] *Çukurova University, Adana, Türkiye*
[139] *Hacettepe University, Ankara, Türkiye*
[140] *Middle East Technical University, Physics Department, Ankara, Türkiye*
[141] *Bogazici University, Istanbul, Türkiye*
[142] *Istanbul Technical University, Istanbul, Türkiye*
[143] *Istanbul University, Istanbul, Türkiye*
[144] *Yildiz Technical University, Istanbul, Türkiye*
[145] *Institute for Scintillation Materials of National Academy of Science of Ukraine, Kharkiv, Ukraine*
[146] *National Science Centre, Kharkiv Institute of Physics and Technology, Kharkiv, Ukraine*
[147] *University of Bristol, Bristol, U.K.*
[148] *Rutherford Appleton Laboratory, Didcot, U.K.*
[149] *Imperial College, London, U.K.*
[150] *Brunel University, Uxbridge, U.K.*

JHEP10(2026)167

[151] The University of Alabama, Tuscaloosa, Alabama, U.S.A.
[152] University of California, Davis, Davis, California, U.S.A.
[153] University of California, San Diego, La Jolla, California, U.S.A.
[154] University of California, Los Angeles, California, U.S.A.
[155] California Institute of Technology, Pasadena, California, U.S.A.
[156] University of California, Riverside, Riverside, California, U.S.A.
[157] University of California, Santa Barbara — Department of Physics, Santa Barbara, California, U.S.A.
[158] University of Colorado Boulder, Boulder, Colorado, U.S.A.
[159] The Catholic University of America, Washington, DC, U.S.A.
[160] University of Florida, Gainesville, Florida, U.S.A.
[161] Florida Institute of Technology, Melbourne, Florida, U.S.A.
[162] Florida State University, Tallahassee, Florida, U.S.A.
[163] Fermi National Accelerator Laboratory, Batavia, Illinois, U.S.A.
[164] University of Illinois Chicago, Chicago, Illinois, U.S.A.
[165] Northwestern University, Evanston, Illinois, U.S.A.
[166] Purdue University Northwest, Hammond, Indiana, U.S.A.
[167] University of Notre Dame, Notre Dame, Indiana, U.S.A.
[168] Purdue University, West Lafayette, Indiana, U.S.A.
[169] The University of Iowa, Iowa City, Iowa, U.S.A.
[170] The University of Kansas, Lawrence, Kansas, U.S.A.
[171] Kansas State University, Manhattan, Kansas, U.S.A.
[172] Johns Hopkins University, Baltimore, Maryland, U.S.A.
[173] University of Maryland, College Park, Maryland, U.S.A.
[174] Boston University, Boston, Massachusetts, U.S.A.
[175] Northeastern University, Boston, Massachusetts, U.S.A.
[176] Massachusetts Institute of Technology, Cambridge, Massachusetts, U.S.A.
[177] Wayne State University, Detroit, Michigan, U.S.A.
[178] University of Minnesota, Minneapolis, Minnesota, U.S.A.
[179] Bethel University, St. Paul, Minnesota, U.S.A.
[180] University of Nebraska-Lincoln, Lincoln, Nebraska, U.S.A.
[181] Rutgers, The State University of New Jersey, Piscataway, New Jersey, U.S.A.
[182] Princeton University, Princeton, New Jersey, U.S.A.
[183] State University of New York at Buffalo, Buffalo, New York, U.S.A.
[184] Cornell University, Ithaca, New York, U.S.A.
[185] University of Rochester, Rochester, New York, U.S.A.
[186] The Ohio State University, Columbus, Ohio, U.S.A.
[187] Carnegie Mellon University, Pittsburgh, Pennsylvania, U.S.A.
[188] University of Puerto Rico, Mayaguez, Puerto Rico, U.S.A.
[189] Brown University, Providence, Rhode Island, U.S.A.
[190] University of Tennessee, Knoxville, Tennessee, U.S.A.
[191] Vanderbilt University, Nashville, Tennessee, U.S.A.
[192] Texas A&M University, College Station, Texas, U.S.A.
[193] Rice University, Houston, Texas, U.S.A.
[194] Texas Tech University, Lubbock, Texas, U.S.A.
[195] Baylor University, Waco, Texas, U.S.A.
[196] University of Virginia, Charlottesville, Virginia, U.S.A.
[197] University of Wisconsin — Madison, Madison, Wisconsin, U.S.A.
[198] An institute or international laboratory covered by a cooperation agreement with CERN
[199] An institute formerly covered by a cooperation agreement with CERN

[a] Also at Yerevan State University, Yerevan, Armenia
[b] Also at Technische Universität Wien, Vienna, Austria
[c] Also at Ghent University, Ghent, Belgium

JHEP10(2026)167

[d] Also at FACAMP — Faculdades de Campinas, Sao Paulo, Brazil
[e] Also at Universidade Estadual de Campinas, Campinas, Brazil
[f] Also at Federal University of Rio Grande do Sul, Porto Alegre, Brazil
[g] Also at The University of the State of Amazonas, Manaus, Brazil
[h] Also at Brandenburg University of Technology, Cottbus, Germany
[i] Also at National and Kapodistrian University of Athens, Athens, Greece
[j] Also at Ecole Polytechnique Fédérale Lausanne, Lausanne, Switzerland
[k] Also at University of Chinese Academy of Sciences, Beijing, China
[l] Also at University of Chinese Academy of Sciences, Beijing, China
[m] Also at School of Physics, Zhengzhou University, Zhengzhou, China
[n] Now at Henan Normal University, Xinxiang, China
[o] Also at University of Shanghai for Science and Technology, Shanghai, China
[p] Also at The University of Iowa, Iowa City, Iowa, U.S.A.
[q] Also at Nanjing Normal University, Nanjing, China
[r] Also at Center for High Energy Physics, Peking University, Beijing, China, Beijing, China
[s] Now at British University in Egypt, Cairo, Egypt
[t] Now at Cairo University, Cairo, Egypt
[u] Also at Purdue University, West Lafayette, Indiana, U.S.A.
[v] Also at Université de Haute Alsace, Mulhouse, France
[w] Also at Ilia State University, Tbilisi, Georgia
[x] Also at Another institute or international laboratory covered by a cooperation agreement with CERN
[y] Also at University of Hamburg, Hamburg, Germany
[z] Also at RWTH Aachen University, III. Physikalisches Institut A, Aachen, Germany
[aa] Also at Bergische University Wuppertal (BUW), Wuppertal, Germany
[ab] Also at Institute for Advanced Simulation — Jülich Supercomputing Centre, Juelich, Germany
[ac] Also at CERN, European Organization for Nuclear Research, Geneva, Switzerland
[ad] Also at HUN-REN ATOMKI — Institute of Nuclear Research, Debrecen, Hungary
[ae] Now at Universitatea Babes-Bolyai — Facultatea de Fizica, Cluj-Napoca, Romania
[af] Also at MTA-ELTE Lendület CMS Particle and Nuclear Physics Group, Eötvös Loránd University, Budapest, Hungary
[ag] Also at HUN-REN Wigner Research Centre for Physics, Budapest, Hungary
[ah] Also at Physics Department, Faculty of Science, Assiut University, Assiut, Egypt
[ai] Also at The University of Kansas, Lawrence, Kansas, U.S.A.
[aj] Also at Punjab Agricultural University, Ludhiana, India
[ak] Also at University of Hyderabad, Hyderabad, India
[al] Also at Indian Institute of Science (IISC), Bangalore, India
[am] Also at University of Visva-Bharati, Santiniketan, India
[an] Also at Institute of Physics, Bhubaneswar, India
[ao] Also at Deutsches Elektronen-Synchrotron, Hamburg, Germany
[ap] Also at Isfahan University of Technology, Isfahan, Iran
[aq] Also at Sharif University of Technology, Tehran, Iran
[ar] Also at Department of Physics, University of Science and Technology of Mazandaran, Behshahr, Iran
[as] Also at Department of Physics, Faculty of Science, Arak University, Arak, Iran
[at] Also at Helwan University, Cairo, Egypt
[au] Also at Italian National Agency for New Technologies, Energy and Sustainable Economic Development, Bologna, Italy
[av] Also at Centro Siciliano di Fisica Nucleare e di Struttura della Materia, Catania, Italy
[aw] Also at James Madison University, Harrisonburg, Virginia, U.S.A.
[ax] Also at Università degli Studi Guglielmo Marconi, Roma, Italy
[ay] Also at Scuola Superiore Meridionale, Università di Napoli 'Federico II', Napoli, Italy
[az] Also at Fermi National Accelerator Laboratory, Batavia, Illinois, U.S.A.
[ba] Also at Lulea University of Technology, Lulea, Sweden
[bb] Also at Consiglio Nazionale delle Ricerche — Istituto Officina dei Materiali, Perugia, Italy

JHEP10(2026)167

[bc] Also at UPES — University of Petroleum and Energy Studies, Dehradun, India
[bd] Also at Institut de Physique des 2 Infinis de Lyon (IP2I), Villeurbanne, France
[be] Also at Department of Applied Physics, Faculty of Science and Technology, Universiti Kebangsaan Malaysia, Bangi, Malaysia
[bf] Also at Trincomalee Campus, Eastern University, Sri Lanka, Nilaveli, Sri Lanka
[bg] Also at Saegis Campus, Nugegoda, Sri Lanka
[bh] Also at Universität Zürich, Zurich, Switzerland
[bi] Also at Stefan Meyer Institute for Subatomic Physics (SMI), Vienna, Austria
[bj] Also at Near East University, Research Center of Experimental Health Science, Mersin, Türkiye
[bk] Also at Konya Technical University, Konya, Türkiye
[bl] Also at Istanbul Topkapi University, Istanbul, Türkiye
[bm] Also at Izmir Bakircay University Faculty of Engineering and Architecture, Izmir, Türkiye
[bn] Also at Adiyaman University, Adiyaman, Türkiye
[bo] Also at Bozok Universitetesi Rektörlügü, Yozgat, Türkiye
[bp] Also at Istanbul Sabahattin Zaim University, Istanbul, Türkiye
[bq] Also at Marmara University, Istanbul, Türkiye
[br] Also at Milli Savunma University, Naval Academy, Istanbul, Türkiye
[bs] Also at The Science and Technological research Council of Türkiye, Informatics and Information Security Research Center, Gebze/Kocaeli, Türkiye
[bt] Also at Kafkas University, Kars, Türkiye
[bu] Now at Istanbul Okan University, Istanbul, Türkiye
[bv] Also at Istanbul University — Cerrahpasa, Faculty of Engineering, Istanbul, Türkiye
[bw] Also at Istinye University, Istanbul, Türkiye
[bx] Also at School of Physics and Astronomy, University of Southampton, Southampton, U.K.
[by] Also at Monash University, Faculty of Science, Clayton, Australia
[bz] Also at Università di Torino, Torino, Italy
[ca] Also at California Lutheran University, Thousand Oaks, California, U.S.A.
[cb] Also at California Institute of Technology, Pasadena, California, U.S.A.
[cc] Also at United States Naval Academy — Physics Department, Annapolis, Maryland, U.S.A.
[cd] Also at Another institute formerly covered by a cooperation agreement with CERN
[ce] Also at Bingol University, Bingol, Türkiye
[cf] Also at Georgian Technical University, Tbilisi, Georgia
[cg] Also at Sinop University, Sinop, Türkiye
[ch] Also at Erciyes University, Kayseri, Türkiye
[ci] Also at Horia Hulubei National Institute of Physics and Nuclear Engineering (IFIN-HH), Bucharest, Romania
[cj] Now at Another institute formerly covered by a cooperation agreement with CERN
[ck] Also at Karamanoğlu Mehmetbey University, Karaman, Türkiye
[cl] Also at Hamad Bin Khalifa University (HBKU), Doha, Qatar
[cm] Also at Yerevan Physics Institute, Yerevan, Armenia
[cn] Also at Imperial College, London, U.K.

JHEP10(2026)167